

An-Najah National University

Faculty of Graduate Studies

**Multifunctional SWCNTs-based co delivery of
silencing gene and Doxorubicin for synergistic
anticancer activity**

By

Noura Sami Ghazal

Supervisor

Dr. Mohyeddin Assali

Co-Supervisor

Dr. Naim Kittana

**This Thesis is Submitted in Partial Fulfillment of the Requirements for
the Degree of Master in Pharmaceutical Sciences, Faculty of Graduate
Studies, An-Najah National University, Nablus, Palestine.**

2019

**Multifunctional SWCNTs-based co delivery of
silencing gene and Doxorubicin for synergistic
anticancer activity**

By

Noura Sami Ghazal

This Thesis was defended successfully on 10/7/2019 and approved by:

Defense Committee Members

Signature

- | | | |
|---------------------------------|----------------------------|-------|
| 1. Dr. Mohyeddin Assali | / supervisor | |
| 2. Dr. Naim Kittana | / co-supervisor | |
| 3. Dr. Hussein Hallak | / External Examiner | |
| 4. Dr. Murad Abu Alhasan | / Internal Examiner | |

Dedication

To the most affectionate and greatest father, mother and grandmother in the world who are supporting me, carrying my burdens, forgiving my mistakes and standing beside me until became what I am now.

To my Sisters Duaa, Marah, and Hiba and my brother Rami.

To my strong pillar Nidal who supported me each step of the way.

To my friends and every person have given me the drive and discipline to tackle any task with enthusiasm and determination.

I dedicate this work

Acknowledgement

Firstly, I thank the holy god for giving me the strength, ability, qualifications and the patience to complete this research.

Then, I want to thank my thesis supervisors: Dr. Mohyeddin Assali for all his support and the valuable guidance and advice in all portion of my research, his willingness to motivate me contributed tremendously to my research. In addition, special thanks to Dr. Naim Kittana for his scientific support, guidance and constructive advice.

I would like to thank the rest of examination committee, for reading my thesis, their insightful comments and suggestions and invaluable criticisms.

Thanks to Hamdi Mango Center for Scientific Research, Faculty of Medicine and Faculty of Science at the University of Jordan for their collaboration in NMR, and TEM measurements.

Special and deepest thanks to the staff of the laboratories of the College of Pharmacy, Science and Medicine for providing help and assistance, especially the supervisor of the laboratories of the College of Pharmacy Mr. Mohammad Arar and the lab workers Tahreer Shtayeh and Linda Arar.

My friends and colleagues in the Department of Pharmacy deserve warm thanks, for their assistance, support and the most beautiful fun time that we spend it together during the period of my study.

My family, which doesn't have any words to express my love, thanks and gratitude to them for their psychological and moral support throughout the years of my studies and work in my research. I hope you will be proud of me.

Noura Ghazal

الإقرار

أنا الموقع أدناه موقع الرسالة التي تحمل العنوان:

Multifunctional SWCNTs-based co delivery of silencing gene and Doxorubicin for synergistic anticancer activity

أقر بأن ما اشتملت عليه الرسالة هو نتاج جهدي الخاص، باستثناء ما تمت الإشارة إليه حيثما ورد، وأن هذه الرسالة ككل، أو أي جزء منها لم يقدم من قبل لنيل أي درجة أو لقب علمي أو بحثي لدى أي مؤسسة تعليمية أو بحثية أخرى.

Declaration

The work provide in this thesis, unless otherwise referenced, is the researcher's own work, and has not been submitted elsewhere for any other degree or qualification.

Student's name:

اسم الطالب:

Signature:

التوقيع:

Date:

التاريخ:

List of Contents

No	Content	Pages
	Dedication	iii
	Acknowledgement	iv
	Declaration	v
	List of tables	ix
	List of figures	x
	List of schemes	xii
	List of abbreviations	xiii
	Abstract	xv
	Chapter One: Introduction	1
1.1	Cancer	1
1.2	Nanomedicine	4
1.2.1	Passive targeting	5
1.2.2	Active targeting	6
1.3	Carbon nanotubes (CNTs)	11
1.4	Functionalization of CNTs	12
1.4.1	Non-covalent functionalization	12
1.4.2	Covalent functionalization	14
1.4.2.1	Oxidation reaction	15
1.4.2.2	Addition reaction	15
1.5	Doxorubicin	16
1.6	Literature Review	17
1.7	Aims of the study	20
1.8	Objectives	21
1.9	General approach of the synthesis and functionalization of SWCNTs	21
	Chapter Two: Reagents and Methods	25
2.1	Reagents and materials	25
2.2	Instrumentation	27
2.3	Synthesis and characterization of the products	27
2.3.1	Synthesis of Tosyl-TEG-OH (1)	28
2.3.2	Synthesis of OH-TEG-N3 (2)	29
2.3.3	Synthesis of COOH-TEG-N3 (3)	30
2.3.4	Synthesis of Boc protected tetraamine (4)	30
2.3.5	Synthesis of Boc-tetraamine-TEG-N3. (5)	32
2.3.6	Synthesis of SWCNTs-alkyne (6)	33
2.3.7	Synthesis of 4-aminophenyl α -D-mannopyranoside (7)	33
2.3.8	Functionalization of SWCNTs-Alkyne with compound 5 (8)	34
2.3.9	Synthesis of f-SWCNTs. (9)	35

2.3.10	Functionalization of SWCNTs-Alkyne with compound 7 (10)	35
2.3.11	Functionalization of f-SWCNTs (10) with compound 5 (11)	36
2.3.12	Deprotection of f-SWCNTs 11 (12)	36
2.3.13	The Quantitative Kaiser Test protocol [that to determine the free NH ₂ loading]	37
2.3.14	Non-covalent functionalization of Dox (13, 14)	37
2.4	In vitro drug release	38
2.4.1	Calibration curve of Doxorubicin HCl using spectrophotometry	38
2.4.2	Calibration curve of mannose using spectrophotometry	38
2.4.2.1	Anthrone method	38
2.5	Anticancer activity	39
2.5.1	Cell line	39
2.5.2	Cell culture	39
2.5.3	Cytotoxicity test	40
2.5.4	Mannose receptor selectivity test	40
2.6	Isolation of RNA	41
2.6.1	Gel electrophoresis experiments	42
2.6.1.1	Composition of FA gel buffers	42
2.6.1.1.1	10x FA gel buffer	42
2.6.1.1.2	1x FA gel running buffer	42
2.6.1.1.3	5x RNA loading buffer	42
2.6.1.2	Formaldehyde Agarose gel	42
2.6.1.3	RNA sample preparation, loading and running	43
2.7	Verification of the primers	43
2.8	Loading PCR samples and running Gel electrophoresis	44
2.9	Knockdown and reverse transfection of β -catenin gene	45
2.9.1	Cell culture	45
2.9.2	Transfection Complex preparation	45
2.9.3	Verification Step (Isolate RNA and perform PCR)	46
2.10	Complexion of f-SWCNT (12) with siRNA	46
2.11	Loading Samples and Running on Agarose Gel	46
	Chapter Three: Results and Discussion	47
3.1	Synthesis and functionalization of SWCNTs	47
3.2	Characterization of Di-f-SWCNTs and Tri-f-mannose-SWCNTs	52
3.2.1	TEM images of the functionalized SWCNTs	52
3.2.2	UV-vis spectrophotometry	53
3.2.2.1	Calibration curve of Doxorubicin	53

3.2.3	Thermogravimetric analysis (TGA)	55
3.2.4	Zeta potential analysis	56
3.3	Cytotoxic activity	56
3.4.1	Concentration and pH-dependent effect on the cytotoxicity of the test compounds	56
3.4.2	Loading mannose on SWCNT and its effect of the cytotoxicity of the test compounds	59
3.5	Evaluation of RNA	61
3.5.1	Quantification of RNA	61
3.5.2	Integrity of RNA	61
3.6	Verification of the primers functionality	62
3.7	Knockdown of β -catenin	62
3.8	Evaluation of f-SWCNT-siRNA Complex formation	63
	Conclusion	65
	Suggestion for future work	66
	References	67
	المخلص	ب

List of Tables

NO	Content	Pages
Table 2. 1	Reaction components for one-step RT-PCR	43
Table 2. 2	Thermal cycler conditions for β -actin	44
Table 2. 3	Thermal cycler conditions for β -catenin	44
Table 2. 4	Thermal cycler conditions for WNT	44

List of Figures

NO	Content	Pages
Figure 1. 1	Variations between normal cell division and cancer cell division [3]	1
Figure 1. 2	carcinogenesis and metastasis process [6]	2
Figure 1. 3	Enhanced permeability and retention (EPR) [12]	3
Figure 1. 4	Non covalent functionalization of CNTs with glycol-nano-materials [80]	13
Figure 1. 5	Covalent functionalization of CNTs [83]	14
Figure 1. 6	Doxorubicin intercalation into DNA. A) Facilitate replication and DNA synthesis by formation of Topoisomerase II (TOP2b) which relaxes DNA supercoil, B) doxorubicin can form a complex by DNA via G bases in two DNA strands and prevents TOP2b activity and DNA synthesis	16
Figure 3. 1	TEM images of A) pristine SWCNTs; B) f-SWCNTs 14	53
Figure 3. 2	Calibration curve of Dox in distilled water at $\lambda_{max} = 485nm$	54
Figure 3. 3	Calibration curve of Mannose in distilled water at $\lambda_{max}=620nm$	54
Figure 3. 4	Thermogravimetric analysis of pristine SWCNTs (black dots) and f-SWCNTs 14 (red dots).	55
Figure 3. 5	Concentration-dependent effect on Caco2 cell viability at different pH values: A) at pH = 7.34, B) at pH = 7.0, C) at pH = 6.5. D) pH dependent effect at a concentration equivalent to 4 mcg/ml Dox. (n=6, *p<0.05, compared to the negative control 0.0 mcg/ml, # p<0.05, compared to the same species concentration at pH = 7.34).	57
Figure 3. 6	: Concentration-dependent effect on MCF7 cell viability at different pH values: A) at pH = 7.34, B) at pH = 7.0, C) at pH = 6.5. D) pH dependent effect at a concentration equivalent to 4 mcg/ml Dox. (n=6, *p<0.05, compared to the negative control 0.0 mcg/ml, # p<0.05, compared to the same species concentration at pH = 7.34).	58
Figure 3. 7	Effect of pre-incubation with mannose on the cytotoxicity of different test substances in Caco2 cell line at a concentration 4 mcg/ml and a pH of 6.5 (n=3, *p<0.05, compared to 0 μ M mannose).	60

Figure 3. 8	Effect of pre-incubation with mannose on the cytotoxicity of different test substances in MCF-7 cell line at a concentration 4 mcg/ml and a pH of 6.5 (n=3, *p<0.05, compared to 0 μ M mannose).	60
Figure 3. 9	Quality assessment for the isolated RNA by agarose gel electrophoresis	61
Figure 3. 10	Figure.3.4: Agarsoe gel electrophoresis subjected to UV light to verify primers	62
Figure 3. 11	Agarsoe gel electrophoresis subjected to UV light to show siRNA transfection of cell lines	63
Figure 3. 12	Agarsoe gel electrophoresis subjected to UV light to visualize free RNA	64

List of Schemes

NO	Content	Pages
Scheme 1	Synthesis of tetra-amine linker	22
Scheme 2	Mono-functionalization of SWCNT with tetraamine linker	23
Scheme 3	Di-functionalization of SWCNT with mannose, and tetraamine linker	23
Scheme 4	:Tri-functionalization of SWCNT with mannose, tetraamine linker, Dox	24
Scheme 5	Synthesis of linker 3 (COOH-TEG-N3)	48
Scheme 6	Synthesis of compound (5)	48
Scheme 7	functionalization of Alkyne-SWCNTs with tetramine spacer	49
Scheme 8	Synthesis of 4-aminophenyl α -D-mannopyranoside	50
Scheme 9	Dual functionalization of SWCNTs to obtain the f-SWCNTs (12)	51
Scheme 10	Non-Covalent functionalization of f-SWCNTs (9) and (12) with Doxorubicin	52

List of Abbreviations

Symbol	Abbreviation
A-549	Human lung adenocarcinoma
Anhydrous CuSO ₄	Anhydrous copper sulfate
CDCl ₃	Deuteriochloroform
CGM	Culture growth medium
CHCl ₃	Chloroform
CNTs	Carbon nanotubes
DCM	Dichloromethane
DDs	Drug delivery systems
DMF	Dimethylformamide
DMSO	Dimethylsulfoxide
DNA	Deoxyribonucleic acid
DOX	Doxorubicin
EDC	Ethylcarbodiimide hydrochloride
EDTA	Ethylene diamine tetra acetic acid
EPR	Enhanced permeability and retention
Et ₃ N	Trimethylamine
FBS	Fetal bovine serum
<i>f</i> -MWCNTs	Functionalized multi-walled Carbon Nanotube
<i>f</i> -SWCNTs	Functionalized single-walled Carbon Nanotube
Hr/s	Hour or Hours
H ₂	Hydrogen gas
H ₂ O	Water
HCl	Hydrochloride
HepG-2	Hepatocellular carcinoma
MCF-7	Human breast cancer cell line
MeOD	Deuteromethanol
MeOH	Methanol
Min	Minutes
MTS	(3-(4,5-dimethylthiazol-2-yl)-5-(3-carboxymethoxyphenyl)-2-(4-sulfophenyl)-2H-tetrazolium)
MW	Molecular weight
MWCNT	Multi-walled carbon nanotube
NIR	Near infrared
NMR	Nuclear Magnetic Resonance
°C	Degree Celsius
<i>o</i> -DCB	Ortho dichlorobenzene
PB	Phosphate buffer
PBS	Phosphate buffer saline

Pd/C	Palladium on carbon
PEG	Polyethylene-glycol
pH	Power of hydrogen
<i>p</i> -SWCNTs	Pristine single-walled Carbon Nanotubes
PNPs	Polymeric nanoparticles
RNA	Ribonucleic acid
siRNA	Small interfering Ribonucleic acid
RPMI	Roswell Park Memorial Institute
SWCNT	Single-walled Carbon Nanotube
TEG	Tetraethylene glycol
TEM	Transmission electron microscope
TFA	Trifluoroacetic acid
TGA	Thermogravimetric analysis
THF	Tetrahydrofuran
TLC	Thin layer chromatography
UV-Vis	Ultraviolet-Visible
λ_{max}	Lambda max

**Multifunctional SWCNTs-based co delivery of silencing gene and
Doxorubicin for synergistic anticancer activity**

By

Noura Sami Ghazal

Supervisor

Dr. Mohyeddin Assali

Co-Supervisor

Dr. Naim Kittana

Abstract

Chemotherapy is a mainstay strategy in the management of cancer. Unfortunately, it can affect healthy cells as the cancerous cells resulting in a number of severe side effects. Therefore, many researchers are trying to develop new drug delivery systems that could reduce the used doses and decrease the side effect. In this field, many efforts have been applied to develop drug delivery systems based on carbon nanotubes. The aim of this work is to develop a new nano-anticancer system based on the multi-functionalization of single-walled Carbon Nanotubes (SWCNTs) using covalent functionalization of SWCNTs with tetraamine spacer and targeting agent, mannose combined non-covalently with doxorubicin on the surface of the *f*-SWCNTs. The characterization of the developed nano-drug was analyzed by transmission electron microscopy which appeared good dispersibility of the functionalized single walled carbon nanotubes which indicates the successful functionalization. Moreover, the percentage of functionalization was determined by thermogravometric analysis obtaining 77.5% of functionalization in the case of *f*-SWCNTs (14). Moreover, the surface charge of the functionalized SWCNTs was +28 mV for the *f*-

SWCNTs (**13**) and +47 mV for the *f*-SWCNTs (**14**) as confirmed by zeta potential analysis.

The cytotoxicity effect of the compounds was studied at different concentrations and different pH conditions and compared with Dox alone. The MTS proliferation assay showed that it could induce greater cytotoxicity at all tested pHs, with the highest effect observed by 4 mcg/ml *f*-SWCNT (**14**) at pH 6.5. After that, the pre-incubation with any of the tested concentrations of mannose reduced the cytotoxicity of Dox-mannose-SWCNT by approximately 96-98%, suggesting that the entry of this complex might be dependent on mannose receptors, which imparts this complex a kind of selectivity for cancer cells that overexpress this type of receptors. Evaluation of RNA in Caco2 cells, Agarose gel electrophoresis demonstrated that the knock-down of β -catenin while using β -actin as a housekeeping gene could promote apoptosis of cells, after knockdown of β -catenin, the gel showed a reduction in the density of β -catenin bands by around 20% as compared with the band of the housekeeping gene β -actin. Finally, the complexion of *f*-SWCNT (**14**) -siRNA exhibits ability to condense RNA at all mass ratios.

Chapter One

Introduction

1.1 Cancer

Cancer is considered the second global reason of mortality after cardiovascular diseases [1], which is term used to express a group of diseases which occur due to out-control cell growth due to multiple changes in the gene expression,

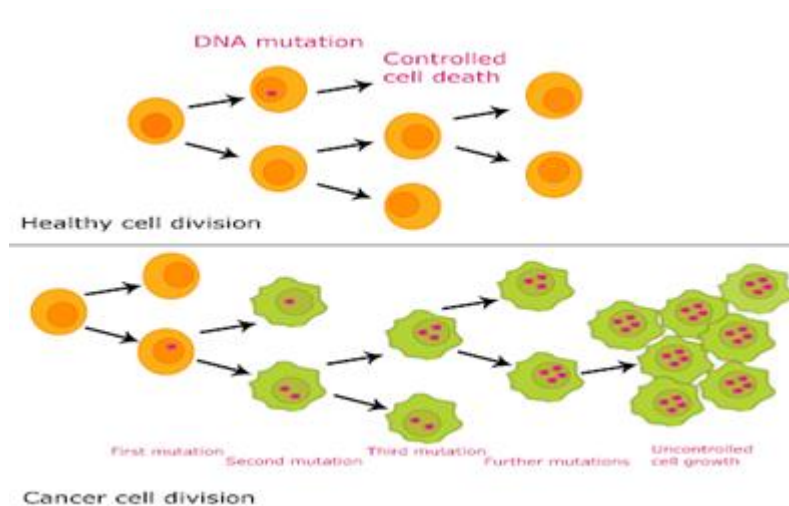


Figure 1. 1: Variations between normal cell division and cancer cell division [3]

Cancer can be classified to benign tumor, and malignant tumor, but the harmful is the malignant, the previous mentioned changes in the gene expression occurs due to several reasons such as carcinogenic chemicals, radiation, viruses, and continuous exposure to these factors leads to development of cancer by proliferation leading to out-control growth, in addition to not responding to the regulatory signals, this process called carcinogenesis [4].

One of the worst characteristic of cancer is metastasis that the cancer cells have ability to spread from the original organ into whole of the body through the lymphatic system and blood circulation, *Figure 1. 2* [5].

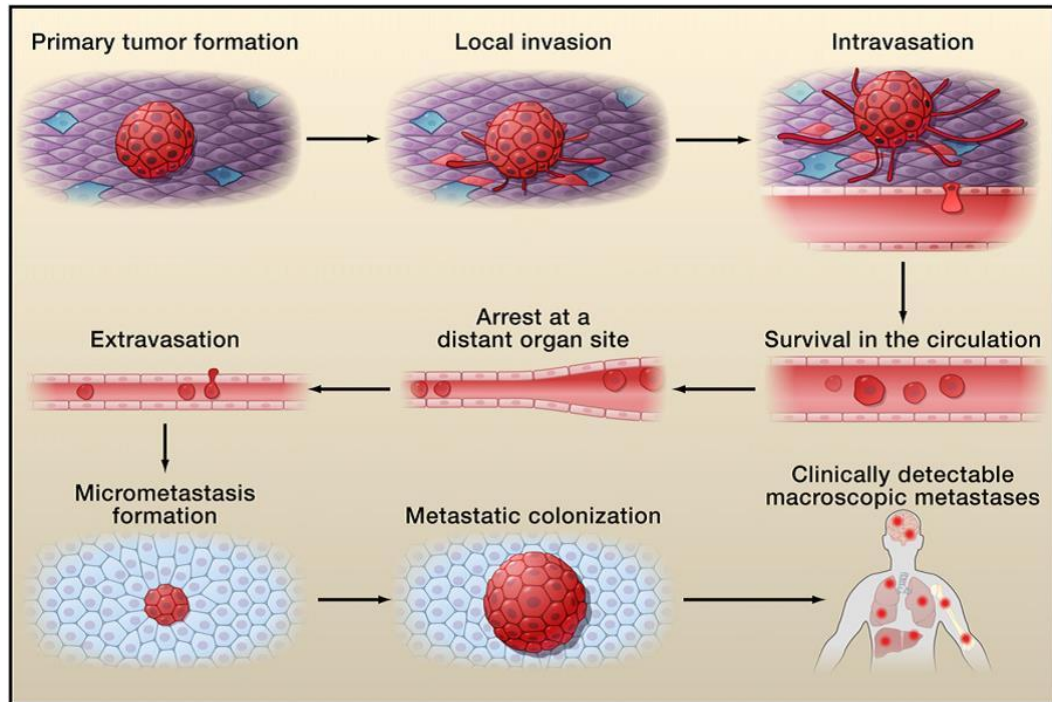


Figure 1. 2: carcinogenesis and metastasis process [6]

Despite other causes, there is a significant factor for the proliferation of cancerous cells, which is to supply cells with nutrients and waste removal, through the creation of new blood vessels, by process called angiogenesis [7]. This process raises an important difference between normal blood vessels and tumor blood vessels, including that they have loose structure, immature and have discontinuous lining of endothelial cells, whole of this make proliferation more rapidly [8, 9].

These differences come back to a phenomenon called enhanced permeability and retention (EPR) effect, which allows blood plasma

components such as, lipid species, macromolecules, and nano-particles to penetrate into tumor cells, this may lead to escape renal clearance and lack of efficient lymphatic drainage, **Figure 1. 3** [10, 11].

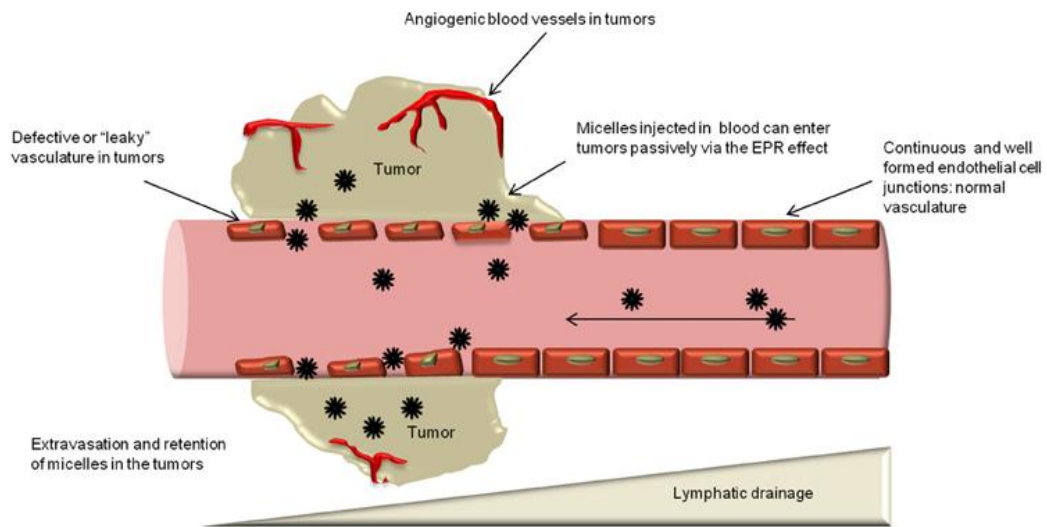


Figure 1. 3: Enhanced permeability and retention (EPR) [12]

Cancer can be treated by surgery, it can be cured if all tumor removed, but this is not always possible. If not removed completely, the cancer will spread into the whole body [13]. Radiation therapy kills cancer cells by using X-ray radiation but it also damages normal cells [14]. Chemotherapy is the usage of cytotoxic drugs (anti-cancer drugs) that can kill cancer cells, most forms of chemotherapy reach all rapidly dividing cells not only cancer cells but these cells usually return into their natural condition after chemotherapy [13]. Hormonal therapy based on providing or blocking certain hormones, this approach used to treat breast and prostate cancers by removing or blocking estrogen or testosterone [15]. Each previous treatment, have common side effect such as bone marrow toxicity,

induction of immunosuppression, fatigue, hair loss, severe pain, burning, numbness, mouth and throat sores, menopausal symptoms in hormonal therapy, radiation recall is a rash that seems like a severe sunburn, it appears when certain types of chemotherapy are given during or soon after treatment by radiation therapy [14, 16-19].

To get rid of side effects of the previous ways, it is necessary to find new methods to be more effective, less harmful to the patients and more tumor selectivity. Therefore, many efforts have been applied in nanomedicine in order to fight against cancer [20].

1.2 Nanomedicine

Nanomedicine has shown obvious benefits in comparison to the traditional chemotherapy such as increase the targeting efficacy, enhanced permeability and retention, improved the half lives and consequently decreases the side effects [20].

To increase targeting efficacy should avoid the traditional delivery system, which allows the drug to reach whole the body through the blood circulation [21, 22], and heading toward targeted drug delivery, which can prolong, target, localize, and protect the drug system [22, 23].

There are two types of targeted drug delivery, passive targeted drug delivery, and active targeted drug delivery.

1.2.1 Passive targeting

In passive targeting, only macromolecules such as nanoparticles accumulate in the neoplastic tissues this occur due to the enhanced permeability and retention (EPR) effect, which is based on two fundamental characteristics, the leaky vasculature and impaired lymphatic drainage of the neoplastic tissues [24, 25].

One year ago, Assali and co-workers developed functionalized SWCNTs covalently with combretastatin A4 (CA4) in the presence of tetraethylene glycol linker through click reaction due to dispersibility improvement, the cytotoxicity of the SWCNT-CA4 was determined by flow cytometry using annexin V/propidium iodide (PI) test, the result suggest that the anticancer activity for novel SWCNT-CA4 higher than free CA4[26].

In 2001, Mitra S and co-workers attempted to couple the doxorubicin with dextran (DEX), then conjugate this drug in hydrogel nanoparticles after encapsulation, the diameter of these nanoparticles was found to be 100 ± 10 nm, which favors the EPR effect, Balb/c mice used to implant the J774A.1 macrophage tumor cells to evaluate the antitumor effect of the system, the results showed that encapsulation reduces the side effects and improves its therapeutic efficacy in mediation of cancer [27].

In 2016, Pan and co-workers developed delivery system based on functionalizing graphene oxide (GO) with fluorescein isothiocyanate, lactobionic acid (LA), and carboxymethyl chitosan (CMC), then adsorption was used to load Doxorubicin (DOX) onto the composites, the

LA-containing composite provides selectively induce the death of cancerous (SMMC-7721) cells despite the LA-free analogue which was inactive, according to these results, the modified GO can be targeted anticancer drug delivery systems because its materials are strong potential candidates [28].

1.2.2 Active targeting

One way to get rid the limitations of passive targeting, which is to attach active targeting agents such as carbohydrates, antibodies, peptides, folic acid or small molecules, nanocarriers will bind to target cancerous cells through ligand–receptor interactions, this occurs through the expression of receptors on the cell surface. But to achieve high specificity, receptors should be over-expressed on cancer cells without the normal cells [25, 29], this conjugation between agents and drug will achieve selectivity to cancer cells and decrease toxicity [30]. The proposed mechanisms of internalization is through receptor-mediated endocytosis, firstly targeting system binds with their receptors, then enclosure around ligand–receptor complex by plasma membrane to form an endosome [25, 29].

One year ago, Khattabi and co-workers developed delivery system based on silica nanoparticles (NPs), the NPs were loaded with melatonin (TQ-MLT) and thymoquinone then conjugated with carboxymethyl- β -cyclodextrin (CM- β -CD) and a long polymer. Then via host guest interaction the folic acid (FA) was embedded into CD cavity, the cell viability assay on HeLa cells confirmed that drug loaded-FA conjugated

NPs have high antitumor effect compared to unconjugated nanoparticles and the free drug [31].

Another study, Yang et al. designed a dual-drug micelle system, they conjugate doxorubicin (DOX) to the poly lactic acid (PLA) end of polyethylene glycol-b-poly lactic acid (PEG-b-PLA), then a ligand of integrin, (cRGDyK) which used as targeting agent was conjugated to the end of PEG. Then via solution-casting method, CA4 was linked to the PEG-b-PLA. The results suggest that the targeting dual-drug micelle system has anti-proliferating, antitumor and apoptosis effect on cancer cell lines [32].

Li Li, et al., designed layered double hydroxide nanoparticles (LDH-based nanocomposite), mannose conjugated onto SiO₂-coated LDH nanocomposite as a targeting moiety for siRNA targeting delivery to tumor cells. According to the data of cellular uptake, which showed that the delivery of siRNA to osteosarcoma cells (U2OS) by using mannose-conjugated SiO₂ which coat LDH nanocomposite to be more efficient compared to unmodified LDH NP, so it provides efficient cancer treatment and huge potentials in cancer therapy [33].

In 2016, Soni and co-workers developed mannosylated solid lipid nanoparticles loaded with Gemcitabine (GmcH) (GmcH-SLNs) due to improving GmcH drug uptake for the lung cancer cells, The cell uptake and cellular toxicity studies were performed and the result appears that the developed nanosystem shows professional targeted delivery of GmcH to

the lung cancer with enhanced safety and improved therapeutic effectiveness [34].

As we see, the most important challenge in using active targeting is selecting the most suitable targeting agents to achieve selectively and successfully transport nanosystems to tumor site and thus avoiding toxicity, so our model will depend on active targeting, and we will use carbohydrates as targeting agent.

Although some tumors of varied types show sugars greediness and elevation of aerobic glycolysis rates, so these cancerous cells may overexpress one or more receptors of different isoforms of carbohydrates to enhance apoptosis [35].

In some types of tumor, lectin-like receptors were overexpressed due to a typical glycosylation that occur in the cell membrane of cancer, and these receptors have huge affinity for different polysaccharides like glucose, galactose, fructose, and mannose [36].

Here, we select mannose receptor, this receptor system able to bind to nano-particles coated with mannose residues, causing rapid internalization of the system within membrane-bound vesicles [37], for example hepatocellular carcinoma (HepG2) and human lung adenocarcinoma (A549) that express mannose receptor and allow active targeting of micelles to cancer cells, which enhance the antitumor efficiency of the drug [38].

Tumorigenesis is related to specific mutations, some of these mutations lead to an imbalance in controlling apoptosis, through overexpression of certain proteins more than normal limit, such as WNT and β -catenin [39]. One of the new trends in cancer treatment is the use of silencing gene siRNA, many studies have reported that the delivery system for gene exhibit a high synergistically therapeutic efficacy, especially in the fields of siRNA [40, 41]. siRNA is a short sequence of RNA that can be used to silence gene expression [42], by the destruction of complementary mRNA by dicer enzyme [43], through RNA interference (RNAi) which is a highly regulated enzyme-mediated process[44], and important in vitro tool to knockdown specific gene, which is anti-apoptotic gene [45]. Here we targeted β -catenin protein and use it as a model.

β -catenin is existing in the nucleus and the cytoplasm. The cytoplasmic β -catenin is one of adherens junctions (AJs) component, and an essential element for stability and cell-to-cell adhesion [46].

β -catenin is a pivotal section of the canonical Wnt/ β -catenin signaling pathway, which is considered as the main cause of human cancers [47], in the absence of Wnt signaling, the level of cytoplasm β -catenin is degraded [48, 49], but in the presence of Wnt signaling, β -catenin will accumulate in the cytoplasm, hence enters the nucleus to form tumors and stimulate proliferation [50, 51].

Generally, β -catenin has many physiological functions, like organ formation and renewal of stem cell, also cell survival and increased growth, enhance invasion and metastatic process, in addition to resistance to chemotherapy [52, 53]. Higher expression of β -catenin and deregulation of Wnt/ β -catenin signaling pathway lead to the more advanced stage of cancer and more poor prognosis [54, 55].

Critical point to success of RNA interference is an efficient siRNA delivery to cancer cells, through viral and non-viral gene delivery, non-viral vectors such as transfection of siRNA by cationic lipid polymer-based transfection reagents [56], electroporation is a physical delivery depends on electrical pulse [57], and viral vectors such as adenovirus, retrovirus, but this system has immune problems and leads to mortality [57].

However, the major current limitations of siRNA delivery lies precisely in the delivery into the interior of the living cell. These limitations are due to, firstly, physicochemical properties of the membrane barriers, siRNA is unstable in the serum and tissues because it is easily digested by nucleases [58]. Secondly, the negative charge and hydrophilicity of free siRNA forbids them from readily crossing cell membranes, therefore, siRNA should be loaded into vesicles in order to taken up by cells [58].

Third barriers is the enzymatic processes, the increase in hydrolytic enzymes such as esterases, nucleases and proteases has a role in the target delivery of siRNA [59].

Lastly, the safety of siRNA is not as expected, it is known that high levels of siRNA may cause activation of innate immune responses and enhance production of cytokines in vivo and in vitro [60, 61].

To avoid these limitations and to disuse the costly and toxic tranfection reagents, huge efforts have been carried out to develop delivery vehicles that are mainly based on nanotechnology [62].

These nanosystems have shown fewer side effects with low immunogenic reactions and are potentially more attractive for clinical applications. However, they have suffered from low loading capacity of the genetic materials; therefore the developing of new nanosystem with high efficacy is still of a high priority.

Many types of nanomaterials were prepared to be applied to medicine such as, polymeric nanoparticles, liposomes, microspheres, micelles, dendrimers and carbon nanotubes (CNTs) [63, 64]. In this project, we are working on carbon nanotubes, therefore the next section will explain in details the characteristics of carbon nanotubes.

1.3 Carbon nanotubes (CNTs)

Among nanotechnology-derived materials, we decided to work with carbon nanotubes (CNTs) which have a significant role in biomedical field because of their unique thermal, mechanical, electrical, and spectroscopic properties [65, 66]. CNTs possess high current carrying capacity which can load various copies of different biological ligands at the same time.

Encouraging feasibility studies have shown the ability of CNTs to be used as delivery systems for peptides, genes, oligonucleotides, cytotoxic drug molecules and antimicrobial agents [67, 68]. CNTs have delivered these macromolecules successfully inside cells by acting as a nano-needle passing the cell membrane without causing any defects [69]. This cell penetration would be very important mechanism to increase the antibiotic concentration inside the microorganism.

1.4 Functionalization of CNTs:

Moreover, recent studies have shown that the functionalization of carbon nanotubes in water with suitable biological groups have a huge effect in enhancement of the biocompatibility, increasing the water solubility, decreasing the toxicity of CNTs and their total elimination from the body without causing any damage [70-72].

1.4.1 Non-covalent functionalization:

The mentioned type of functionalization happens because of Van der Waals interaction among molecules and carbon nanotubes, such as, polymers, surfactants, and aromatic compounds could use to modulate the surface of nanotubes [73-75]. The benefit of non-covalent functionalization is maintenance the electrical characteristics of CNTs, but still sensitive to environmental conditions like salt concentration and pH. Therefore, the drugs that were loaded on the surface of CNTs may release before reaching the target site [76]. Accordingly, they was evaluated the case of using

aromatic compounds which interact with the surface of CNTs through π - π stacking interactions [77-79].

In this way, Assali et al. have promoted a new approach to increase the biocompatibility of Nano-materials via non-covalent functionalization of neoglycolipid compound on the CNTs surface by using π - π stacking interactions, **Figure 1. 4**.

They aimed to synthesize neo-glyco-conjugates structure (compound I), this compound is a pyrene tail linked to the glycol-ligand (sugar head) by the spacer, then tetra ethylene glycol was attached to enhance hydrophilic/hydrophobic balance. other ligand-lectin interactions like glycol conjugation on the cell membrane could be attracted by this aggregates [80].

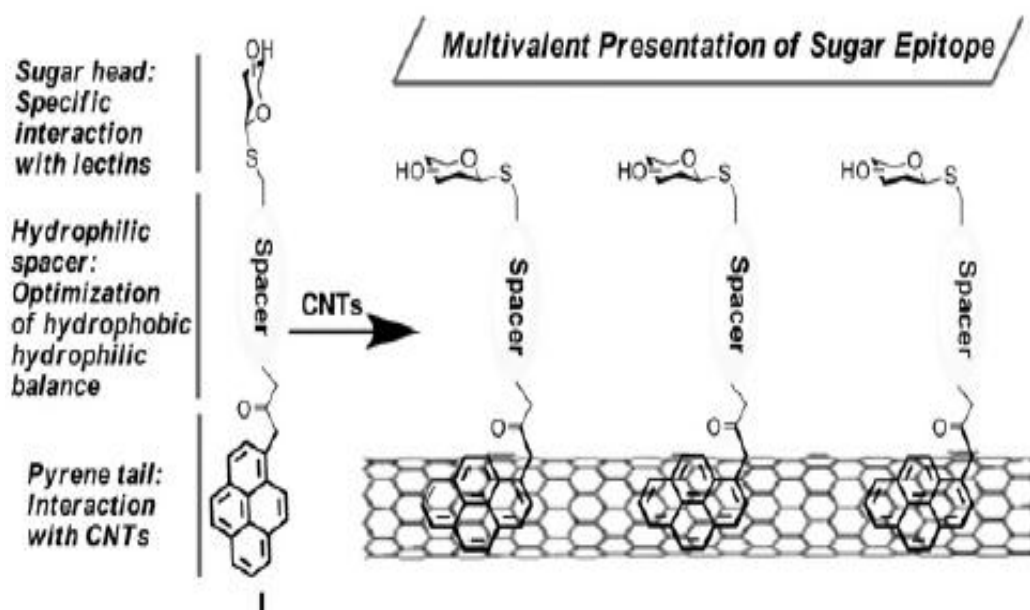


Figure 1. 4: Non covalent functionalization of CNTs with glycol-nano-materials [80]

1.4.2 Covalent functionalization:

The ability of synthesis Covalent chemical combinations can be achieved through different reactions, such as, oxidation reaction [81], addition reactions, arylation [82] and others, **Figure 1. 5** [83, 84]. Interest of covalent functionalization is alteration of electrical characteristics of CNTs as a result to change the hybridization of carbon from sp^2 to sp^3 . This type of functionalization aimed to prevent the release of the attached biomolecules until reaching the target site so declines the side effects of these biomolecules [85, 86] . In the next section, the addition reaction and the oxidative functionalization will be discussed as they were used in the thesis.

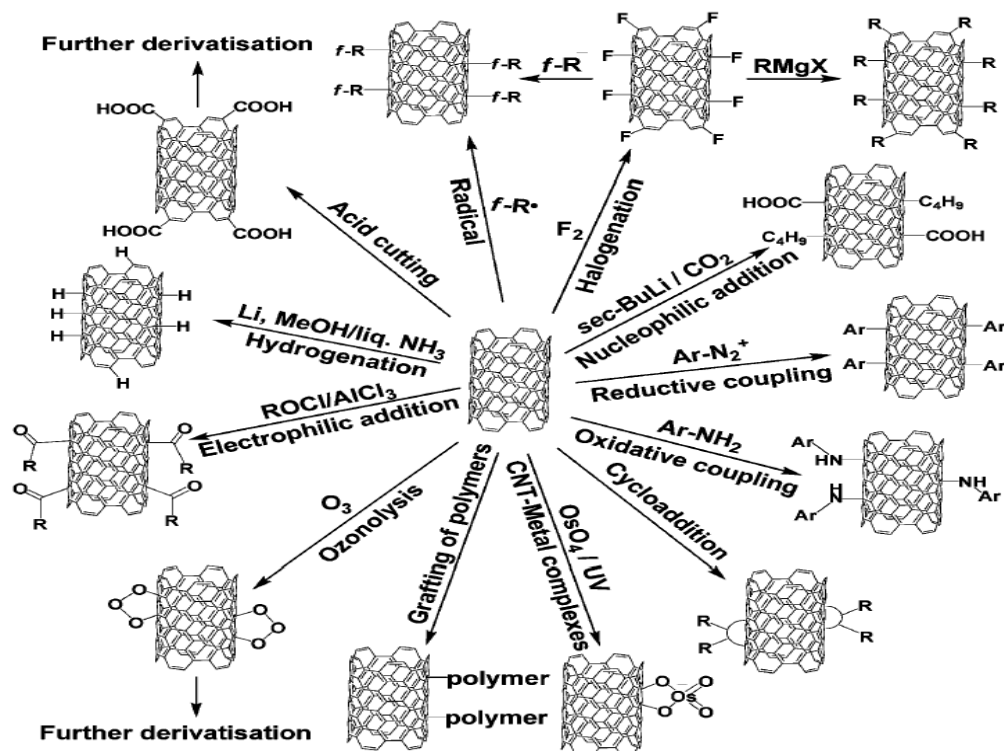


Figure 1. 5: Covalent functionalization of CNTs [83].

1.4.2.1 Oxidation reaction:

To oxidize CNTs, strong oxidative and acidic conditions must be available, such as mixture of strong acids joined with sonication or heating that allowed the open tubes to be shorter and decorated with oxygenated functions, which are prominent on the tips. Different groups introduced on the surface of CNTs, for example (hydroxyl, carbonyl, carboxyl, etc.), these functional groups are exploited as linker for amidation or esterification reactions [85].

1.4.2.2 Addition reaction:

This reaction leads to covalent functionalization by alter the hybridization of carbon from sp^2 to sp^3 . These alterations are associated with generation of tetrahedral geometry by changing the predominantly trigonal-planar local bonding geometry. There are many types of addition reactions such as cycloaddition, fluorination, radical additions, electrophilic and nucleophilic additions [85]. Tour et al functionalized SWCNTs by loading reduced aryl diazonium salts through electrochemical reaction. By using one-electron reduction, the diazonium salts were converted to the aryl radicals [82]. The resulting materials showed good-dispersibility in both water and organic solvents [87].

1.5 Doxorubicin:

Doxorubicin (DOX) is isolated from *Streptomyces peucetius* cultures, and is a cytotoxic anthracycline antibiotic with a molecular formula $C_{27}H_{30}ClNO_{11}$ and a molecular weight 580 [19, 88, 89]. Doxorubicin is a hygroscopic crystalline powder with orange red color. It is slightly soluble in methanol and soluble in water [88]. Doxorubicin used as chemotherapeutic agents, because it is one of DNA intercalating agents. The mechanism of action is based on breakage of double strand of DNA and subsequently prevent the ligation of the nucleotide strand, this occurs through formation of topoisomerase II which is a cleavable complex, leading to apoptosis of cells, **Figure 1. 6** [90-92].

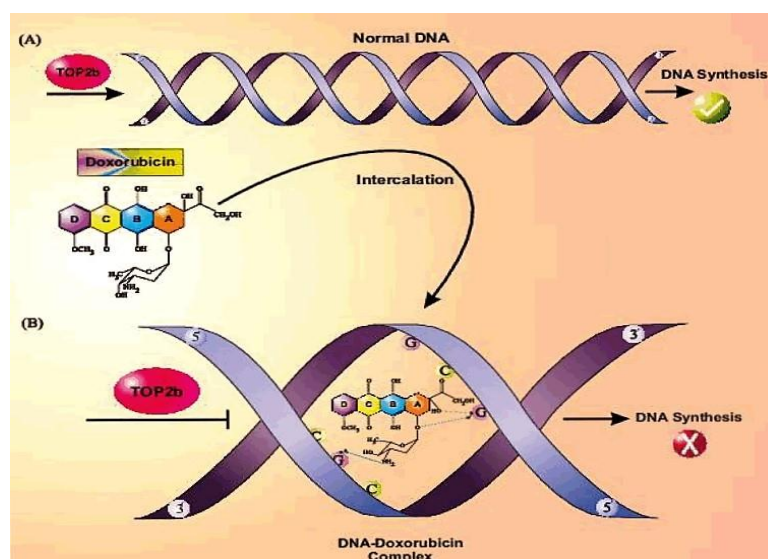


Figure 1. 6: Doxorubicin intercalation into DNA. A) Facilitate replication and DNA synthesis by formation of Topoisomerase II (TOP2b) which relaxes DNA supercoil, B) doxorubicin can form a complex by DNA via G bases in two DNA strands and prevents TOP2b activity and DNA synthesis.

DOX is used to treat broad species of solid tumors like thyroid, bladder, endometrium, stomach, ovary, breast and bone sarcomas. Also, it can be used in the treatment of acute myeloblastic leukemia's and lymphoblastic, as well as lymphoma [90]. However, due to the huge side effects of DOX including alopecia, gastrointestinal disorders, stomatitis, cumulative cardiotoxicity and bone marrow toxicity, the use of DOX is decreased [93].

As mentioned early, the pH value of solid tumors is 7.2-7.4, it will be dropped significantly in the intracellular compartment to 4.0-6.5 [94]. Therefore, this feature can be exploited, by coupling drug to carrier via acid sensitive bond for intracellular drug delivery system.

In order to decrease the toxicity and the side effects of the drug, the most amount of drug must be more concentrated in the tumor cells only. Creating a carrier system and utilization of specific targeting agent can improve the bioavailability of a drug, its water solubility and maintain the tumor apoptosis effect with minimum level of side effects.

1.6 Literature Review:

Many attempts were carried out in order to improve the safety and efficacy of the anticancer agents using different types of nano-systems such as nanoparticles, liposomes, micelles and others. In this literature review, mannose, DOX and siRNA conjugated with nanomaterials were mainly reported.

Recently, Assali and co-workers aimed to functionalize single walled carbon nanotubes with Doxorubicin by adding tetraethylene glycol linker for solubility and dispersibility improvement, then use mannose as targeting agent to reach cancer cell so mannose was also loaded on the surface of nano-system, after tested, the cytotoxicity of Dox-mannose-SWCNT was reduced by approximately 40-57%, and the entry of this complex depends on mannose receptors, which provides this nanosystem selectivity for cancer cells [95]

Sun and et al., developed a potential gene-delivery system of polyethyleneimine and triethyleneglycol polymer which used as cross-linker to form (PEI-TEG) in addition to a series of its mannosylated derivatives, PEI-TEG was synthesized, then connected to mannose through a bridge of phenylisothiocyanate to get man-PEI-TEG conjugates. Particle size, DNA-binding abilities and zeta potential were measured to evaluate the abilities of DNA conveyance of man-PEI-TEG, and PEI-TEG, according to PEI25k as a control. They were retained the superior characterization of PEI25k for a purpose of condensing DNA. The in vitro transfection efficiency, cell uptake, and cytotoxicity of these PEI/DNA complexes were studied using DC2.4 cell line. The results were shown that man-PEI-TEG performed better in both transfection assays and cellular uptake, and had less cytotoxicity in vitro. Finally, they conducted a maturation experiment using flow cytometry in order to evaluate the costimulatory molecules CD40, CD80, and CD86 effect on murine bone marrow-derived DCs (BMDCs). The results of last experiment showed that

for DC maturation, all the PEI/DNA complexes induced a sufficient up-regulation of surface markers. The results obtained were elucidated that man-PEI-TEG can be considered as a DC-targeting gene-delivery system [96].

Kima and et al, developed a delivery system special for siRNA consists of cationic polyethylenimine (PEI) to compact and complex with siRNA, polyethylene glycol (PEG), added for steric stabilization which form a hydrophilic coat outside of the polyplex, pegylation process of the PEI decreased toxicity without any effect on the efficiency of knockdown relative to PEI alone, and mannose (Man) acts as a ligand for cell binding for macrophages, the PEI-PEG. Mannosylation may be executed without any considerable lowering in the efficiency of the knockdown relative to PEI alone. In case of conjugating mannose through the PEG spacer to PEI created higher level of gene knockdown activity and toxicity relative to PEG and conjugating mannose directly to the PEI backbone.

The resultant delivery system was generated in two varied routs. First one, PEG chains and mannose are conjugated to the PEI backbone directly. Other way, conjugation the end of the PEG chain, one end to mannose and the other end to the PEI backbone. Scanning Electron Microscopy (SEM) images PEI-PEG-Man-siRNA polyplexes were done, and showed a coarse surface, sizes of polyplex were found from 169 to 357 nm. PEI-PEG-mannose polymers can complex with siRNA efficiently at low N/P ratios according to Gel retardation assays. The PEI-PEG-Man-siRNA polyplexes

may enter the cells and localized at 2 h post-incubation in the lysosomes according to confocal microscope images [97].

Ali Mohammadi et al., functionalization of SWCNTs with chitosan, Palmitoyl Chitosan and Carboxymethyl Chitosan for targeting drug delivery of doxorubicin, an anti-cancer drug. Chitosan, palmitoyl chitosan and carboxymethyl chitosan have been applied to functionalization of carbon nanotubes, then, doxorubicin was loaded and finally, folic acid was attached by covalent interaction for improving the capabilities of carrier targeting. Whole drug delivery systems showed excellent stability under physiological conditions, and the maximum release was for DOX-CS-SWCNT (20% after 72 h) occurred while simulating the cancer cell condition pH 5.5, the DOX in DOX-CS-SWCNT was efficiently released (70%). Moreover, attachment of folic acid as a targeting agent increases cytotoxicity since the cell viability after 72 h of DOX-NPCS-SWNT was higher than that of FA-DOX-NPCS-SWNT (20%) [98].

From this literature review, it is noticed that there is no previous reports on triple functionalization of SWCNTs with Dox, targeting agent and siRNA.

1.7 Aims of the study

Herein, the aim of this project is to develop a new multi-delivery system of single walled carbon nanotubes (SWCNTs) loaded with Doxorubicin (Dox) as an anticancer drug, siRNA against selected antiapoptotic gene/s which candidates in breast cancer and colorectal adenocarcinoma is β -catenin and a specific targeting agent such as mannose will be attached to the nano-

system, in order to increase its selectivity on the cancer cells and to derive the cancer cells to apoptosis.

1.8 Objectives

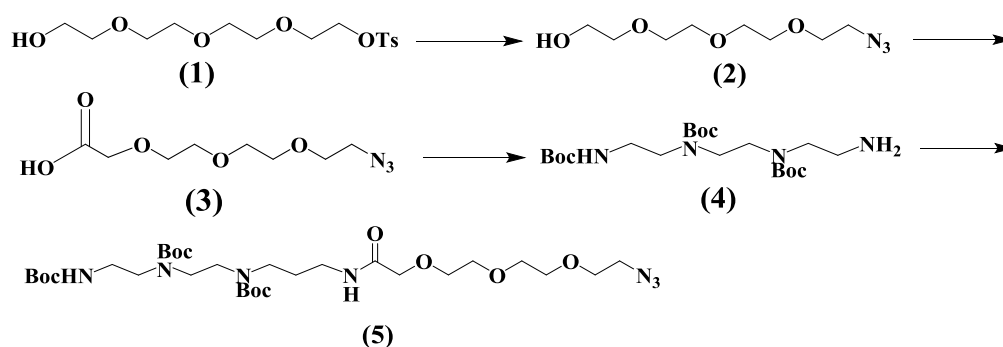
1. The high multi-functionalization of SWCNTs with a derivative of polyamines in order to hybridize with siRNA, targeting agent and non-covalently with Dox.
2. Characterization of the developed nanosystem by various analytical techniques such as TEM, TGA, zeta potential analysis and UV-Vis spectroscopy in order to identify the morphology, size, stability, and the quantity of the multi-functionalized SWCNTs.
3. Tests the successful hybridization of siRNA with the multi-functionalized SWCNTs.
4. Test the In vitro anticancer activity of the developed multi nano delivery system and comparing the results with the individual therapy.

1.9 General approach of the synthesis and functionalization of SWCNTs

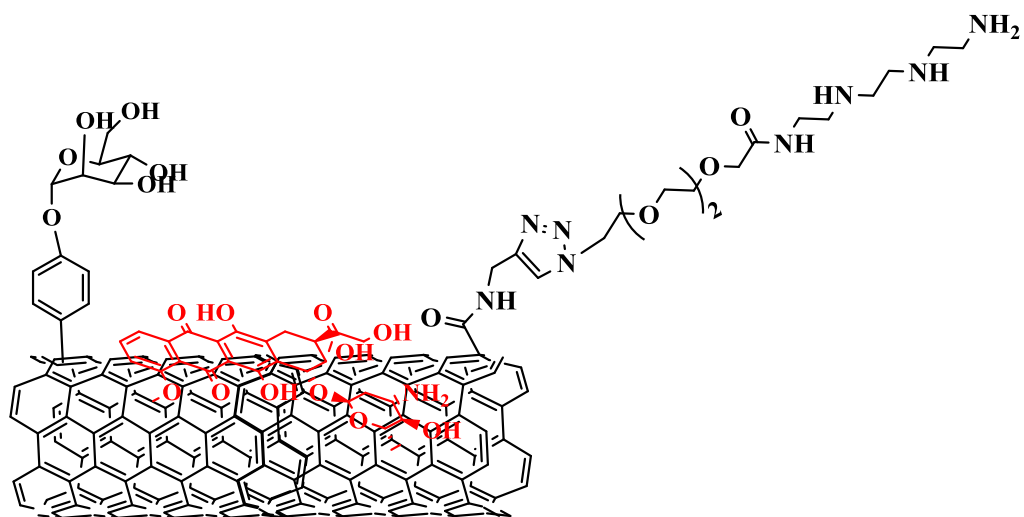
In this thesis we aim to have mono-functionalization of SWCNTs with tetramine linker, bi-functionalization with tetramine linker and mannose as targeting agent. Finally, tri-functionalization with tetramine linker, mannose and Doxorubicin.

For mono-functionalization, the SWCNTs-alkyne was clicked with the prepared tetramine linker through click reaction as shown in **Scheme 1** and **Scheme 2**.

For di-functionalization, the mannose was added to the surface of the SWCNTs-alkyne through diazonium functionalization. After that, the tetramine linker was added through click reaction as shown in **Scheme 3**. Finally, for the tri-functionalization, Doxorubicin was incubated with the di-functionalized SWCNTs in order to be absorbed non-covalently on the surface of the SWCNTs as shown in **Scheme 4**.



Scheme 1: Synthesis of tetra-amine linker.



f-SWCNTs (14)

Scheme 4: Tri-functionalization of SWCNT with mannose, tetraamine linker, Dox.

Chapter Two

Reagents and Methods

2.1 Reagents and materials

1-(3-Dimethylaminopropyl)-3-ethylcarbodiimide hydrochloride (EDC) (catalog # A10807), propargylamine (catalog # H53495), 4-nitrophenyl- α -D-mannopyranoside (catalog # N01C012), trifluoroacetic acid (TFA) (catalog # A12198), TBTU (catalog # B23597) and tetraethylene glycol (TEG) (catalog # B23990) were purchased from Alfa Aesar company (England). Sodium azide (catalog # 0E30428) and 1,2-Dichlorobenzene (*o*-DCB) (catalog # 65152) were purchased from RiedeldeHaën Company (Germany). Mannose (catalog# SLBH1709V), Doxorubicin HCl (catalog # LRAB2383), toluene-4-sulfonylchloride (catalog # 1234411), palladium on carbon (catalog # 101375286), and iso-amyl nitrite (catalog # 110463) were purchased from (Sigma-Aldrich, USA). *N,N*-diisopropylethylamine (DIPEA) (catalog # 496219), ethyl trifluoroacetate (catalog # A821163), 4-(dimethylamino) pyridine (DMAP) (catalog # 1122583), di-tert-butyl dicarbonate (BOC₂O) (catalog # 101281549), and Silica gel were purchased from (Sigma-Aldrich, USA). Triethylenetetramine, 60% (catalog # 34407) was purchased from (ACROS Organics™). Acetone, ethanol (EtOH), methanol (MeOH), dichloromethane (DCM), and isopropyl alcohol were purchased from (C.S. Company, Haifa). Chloroform (CHCl₃) (catalog # 67-66-3), triethylamine (Et₃N) (catalog # 40502L05) and diethyl ether (catalog # 38132) were purchased from (Merck Millipore) and tetrahydrofuran (THF) solvent (catalog # 487308) was purchased from

(Carlo Erba Company, MI. Italy). *N*-Dimethylformamide (DMF) (catalog # 55145) was purchased from (Frutarom Laboratory Chemicals). Anthrone, disodium hydrogen phosphate, sodium chloride, sodium hydroxide and potassium dihydrogen phosphate were purchased from (C.S. Company, Israel). *n*-hexane (Hex) (catalogue # 2355544800024) and acetonitrile (CH₃CN) (catalogue # 5550070) solvents were purchased from (Frutarom Company, Haifa). Carboxylated SWCNTs (Catalog # 99685-96) was purchased from nanostructured and amorphous materials, Inc USA. PTFE-Filter (Sartouris Stedim Biotech GmbH 37070 Gottingen, Germany). TLC (DC-FertigfolienAlugeram®Silg/Uv254, Macherey Nagel Company, Germany), aqueous phosphomolybdic acid hydrate (catalog # 221856), were purchased from (BD Company, USA).

For biological test, Dulbecco's free Ca⁺⁺ -phosphate buffered saline (REF # 02-023-1A) and L-glutamine solution (REF # 03-020-1B), Pen-Strep Solution (catalog # 030311B) were purchased from (Biological industries, Jerusalem). RPMI (catalogue # 05669) was purchased from (Manassas VA, USA), Trypsin-EDTA solution 1X (catalog # 59417C), fetal Bovin Serum (catalog # C8065) and trypan blue solution (catalog # RNBD6249), MOPS (catalog # M9381), Triazol Reagent (catalog # T46108) and Agarose (catalog # A2790) were purchased from (sigma-aldrich, USA). β-catenin siRNA (lot # F2918). QIAGEN Onestep RT-PCR Kit. Ethidium Bromide (lot # 276321) was purchased from hylabs. MTS (catalog # G3581) purchased from (Promega, USA).

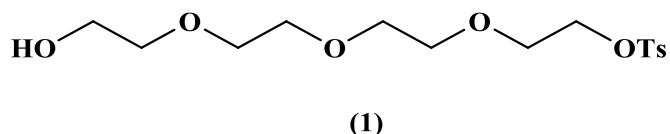
2.2 Instrumentation

NMR analysis was measured by Bruker Avance 500 spectrometer at Jordan University. Absorption analysis was conducted on (7315 Spectrophotometer, Jenway, UK) using 10-mm quartz cuvettes. Water bath and Sonicator (Elmasonic S 70 H, Elma®, Germany). Rotary Evaporator (MRC, ROVA-100, laboratory equipment manufacturer). Centrifuge (UNIVERSAL 320, HettichZentrifugen, Germany). Centrifuge-DCS-16-RVT (Prevac, Canada), used for 4 °C. PCR (Prime Thermal Cycler, Bibby Scientific Ltd, Britain). Esco celculture CO₂ incubator was used to incubate cell line. Accumax Variable micropipette, UK was used for pipetting. TGA analysis was achieved on TAQ50 instrument with a flow rate 50 cc/min under nitrogen with a range 25-600 °C. TEM images were done on FEI Morgagni at Jordan University. FTIR analysis was done on Nicolet iS5, ThermoFisher Scientific Company, USA. Unilab microplate reader 6000 (was used to read the plate for cell viability test).

2.3 Synthesis and characterization of the products:

All the synthetic procedures and anticancer activity were prepared at An-Najah University laboratories. NMR and TEM measurements were conducted at the University of Jordan.

2.3.1 Synthesis of Tosyl-TEG-OH (1)



Compound (1) was synthesized as published previously in our research group[26].

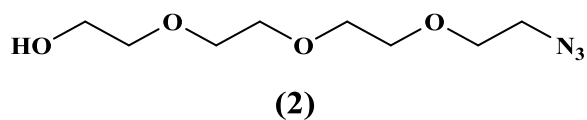
Tetraethylene glycol (10 g, 51.5 mmol), Et₃N (7 ml, 51.5 mmol) was added to 40 ml THF, the mixture was stirred for 5 min, then tosyl chloride (10 g, 52.5 mmol) was added to the rxn gradually at ice bath over a period of 30 min. The reaction was stirred overnight at room temperature. The obtained product was diluted by CHCl₃ (200 mL), then washed with HCl 1M (50 mL) and brine (50 mL). The excess solvent was removed under vacuum and the remaining crude product was purified by flash chromatography on silica gel, eluting with CHCl₃/MeOH (20:1) to give a pale yellow oil. The yield was 36% (4 g, 14.3 mmol).

R_f: 0.5(CHCl₃/MeOH 9:1)

¹H NMR (400 MHz, CDCl₃): δ 7.77 (d, 2H, J = 8.3 Hz, Ts), 7.33 (d, 2H, J = 8.0 Hz, Ts), 4.13 (t, 2H, J = 4.7 Hz, CH₂OTs), 3.66 (t, 2H, J = 4.9 Hz, CH₂CH₂OTs), 3.57-3.56 (m, 8H, 4CH₂O), 3.50 (t, 2H, J = 5.2 Hz, CH₂CH₂OH), 3.27 (s, 2H, CH₂OH).

¹³C NMR (100.6 MHz, CDCl₃): δ 144.8 (2CH Ar), 133.0 (2CH Ar), 129.8 (C Ar), 127.9 (C Ar), 70.7, 70.5, 70.2, 70.1 (CH₂CH₂OH), 69.2 (CH₂OTs), 68.6 (CH₂CH₂OTs), 40.3 (CH₂OH).

2.3.2 Synthesis of OH-TEG-N₃ (2)



Compound (2) was synthesized as published previously in our research group[26].

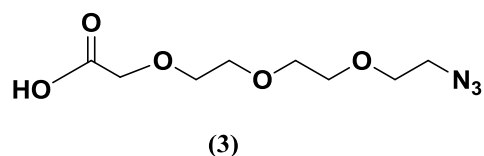
To a solution of compound 1 (1.4 g, 4.02 mmol) dissolved in 6 ml EtOH, sodium azide (287.4 mg, 4.42 mmol) was added. The reaction was stirred in reflux at 70 °C overnight. After removing of EtOH under vacuum, the reaction was diluted with diethyl ether (100 ml) and washed with brine (40 ml). The solvent was removed under vacuum to give a pale yellow oil product. The obtained yield was 85% (1.23 g, 5.6 mmol).

R_f: 0.39 (DCM/MeOH 20:1)

¹H NMR (500 MHz, CDCl₃): δ 3.58 (t, 2H, J= 4.8 Hz, HOCH₂CH₂), 3.55-3.51 (m, 10H, 5 CH₂O), 3.46 (t, 2H, J = 4.8 Hz, OCH₂CH₂N₃), 3.26 (t, 2H, J = 4.8 Hz, CH₂CH₂N₃), 3.10 (bs, 1H, OH).

¹³C NMR (125.7 MHz, CDCl₃): δ 72.5 (HOCH₂CH₂O), 70.6, 70.5, 70.4, 70.2, 69.9 (CH₂O), 61.5 (COH), 50.5 (CN₃).

2.3.3 Synthesis of COOH-TEG-N₃ (3)



Compound (3) was synthesized as published previously in our research group[26].

To a solution of compound 2 (450 mg, 2.05 mmol) dissolved in 15 ml chronic acid, and 15 ml acetone. The reaction was stirred 2-3 hr. After that, isopropanol was added drop by drop to the rxn until the color converted to blue. The rxn was filtered with small silica gel. The solvent was evaporated. The obtained yield was 95% (342 mg, 1.45 mmol).

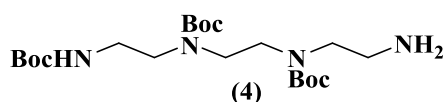
R_f: 0.4 (DCM/MeOH 9:1).

¹H NMR (500 MHz, CDCl₃): δ 9.30 (bs, 1H, COOH), 4.15 (s, 2H, CH₂COOH), 3.80-3.60 (m, 10H, 5CH₂O), 3.29 (t, 2H, J = 4.5 Hz, CH₂N₃).

¹³C NMR (125.7 MHz, CDCl₃): δ 173.5 (CO), 70.9 (CH₂COOH), 70.4, 70.3, 70.2, 69.9, 68.3 (OCH₂CH₂N₃), 50.5 (CN₃).

IR: broad peak (2200-2600), 2921.63, 2853.17, 2108.78, 1714.41 cm⁻¹.

2.3.4 Synthesis of Boc protected tetraamine (4)



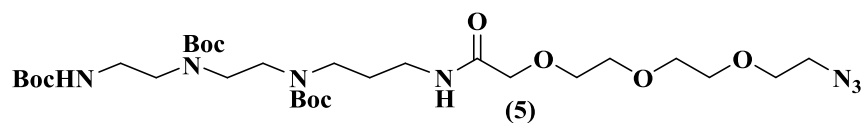
A volume of 70 ml dry methanol was added to triethylenetetramine (745 μl, 4.99 mmol) under argon. Ethyl trifluoroacetate (995 μl, 4.99 mmol) was

added for reaction drop by drop for 45 min on dry ice (-78 °C). After that, remained in dry ice for another 45 min. Then the reaction was remained for an hour at 0 °C. Boc₂O (4.0 g, 18.3 mmol) was mixed with 10 ml dry methanol and added drop by drop, the reaction remained on stirrer overnight. Methanol was removed and the powder was diluted with 60 ml DCM. Then the reaction was extracted by a solution of NaHCO₃ (100 mg) in 40 ml distilled water and dichloromethane layer was dried using (Na₂SO₄), filtered and then DCM was evaporated. The product was white powder. TLC was visualized by (DCM: MeOH: NH₄OH (10:1:0.1)), yield (72%), (1.8 g, 8.2 mmol). After that, product was crystallized using DCM/Hexane to obtain white solid. Then the powder was dissolved in 70 ml methanol and (580 mg K₂CO₃ in 5 ml distilled water). The reaction was running on stirrer at 70 °C for 6 hours. Methanol was evaporated and 150 ml of dichloromethane and 50 ml of distilled water was used for extraction. Dichloromethane dried by using (Na₂SO₄), then filtered and evaporated. The reaction was purified by using flash chromatography (DCM: MeOH: NH₄OH (10:1:0.1)) to provide triethylenetetramine-Boc compound. Yield (44 %) (1.0 g, 2.24 mmol).

R_f: 0.48 (DCM: MeOH: NH₄OH (10:1:0.1)).

¹H NMR (500 MHz, CDCl₃): δ 3.35 – 3.20 (bm, 10H, 4CH₂N & CH₂NH), 2.68 (bt, 2H, CH₂NH₂), 1.41 (s, 27H, C(CH₃)₃), 1.35 (s, 2H, NH₂).

2.3.5 Synthesis of Boc-tetramine-TEG-N₃. (5)



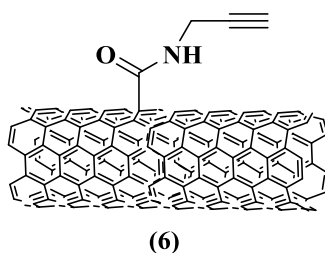
Compound (4) (150 mg, 0.3 mmol), and DIPEA (86 mg, 0.67 mmol) was added under argon, then a solution of compound (3) (90 mg, 0.36 mmol), DIPEA (86 mg, 0.67 mmol) and TBTU (169 mg, 0.44 mmol) was added in acetonitrile. Then reaction was put on stirrer for 24 hr at room temperature. The reaction was diluted with 70 ml of dichloromethane and washed by 30 ml of 1M HCl. DCM layer was dried over drying agent (Na₂SO₄). The obtained product was pale yellow oil. TLC was visualized by (DCM: MeOH (15:1)). The reaction was purified by using flash chromatography (DCM: MeOH (15:1)). The obtained yield was 89% (240 mg, 0.36 mmol).

R_f: 0.5 (DCM: MeOH (15:1)).

IR: 2105.28, 3345.60, 2928.01, 1688.25 cm⁻¹.

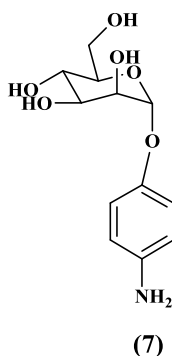
¹H NMR (500 MHz, CDCl₃): δ 3.96 (s, 2H, CH₂CONH), 3.68-3.64 (m, 8H, 4CH₂O), 3.39-3.24 (m, 16H, 4CH₂N, 2CH₂NH, COCH₂CH₂N₃ & COCH₂CH₂O), 2.2 (t, 2H, J = 4.4 Hz, CH₂N₃), 1.44 (s, 27H, C(CH₃)₃).

2.3.6 Synthesis of SWCNTs-alkyne (6)



30 mg of carboxylated SWCNTs was dissolved in DMF (30 ml). Then EDC (15.0 mg, 0.08 mmol) and Et₃N (150 μl, 1.09 mmol) were added. Then the mixture was sonicated for 1hr, and propargylamine (25 μl, 0.41 mmol) was added. After that the mixture was sonicated for 10 min then stirred for 72hr under argon. Then 25 ml CHCl₃ was added to the reaction, filtered under vacuum with CHCl₃ (2 x 20 ml), then with DCM (10 ml) and lastly with diethyl ether (2 x 20 ml). The black powder was collected and the resultant product was 28 mg.

2.3.7 Synthesis of 4-aminophenyl α-D-mannopyranoside (7)



4-nitrophenyl α-D-mannopyranoside (100 mg, 0.37 mmol) dissolved in 5 ml Milli Q water, 10 mg Pd/C was added after sonication for 10 min. The reaction was put on stirrer overnight under H₂ bubbling at room temperature. Then the reaction was filtered using silica gel and washed

with EtOH. The solvent was removed under vacuum to give yellowish brown sticky product. (Yield 99%, 84 mg, 0.37 mmol).

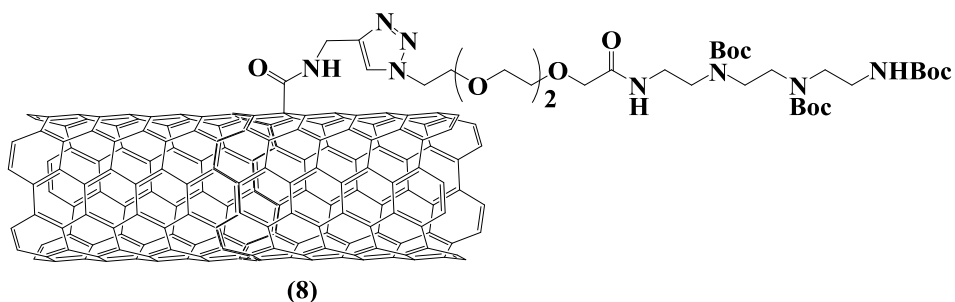
R_f : 0.25 (DCM/MeOH 9:1).

IR: 2939.51, 2851.22, 1649.85, 3319.28 cm^{-1}

^1H NMR (500 MHz, MeOD): δ 6.82 (d, 2H, $J = 9.2$ MHz), 6.55 (d, 2H, $J = 8.7$ MHz), 5.32 (s, 1H; H-1), 3.98 (m, 1H), 3.85 (dd, 1H, $J = 9.0$ MHz, $J = 2.8$ MHz), 3.73 (dd, 1H, $J = 11.3$ MHz, $J = 2.2$ MHz), 3.71-3.73 (m, 2H), 3.62-3.65 (m, 1H);

^{13}C NMR (125 MHz, MeOD): δ 149.7, 143.1, 118.2, 116.8, 101.0, 74.0, 72.2, 72.0, 67.3, 61.9.

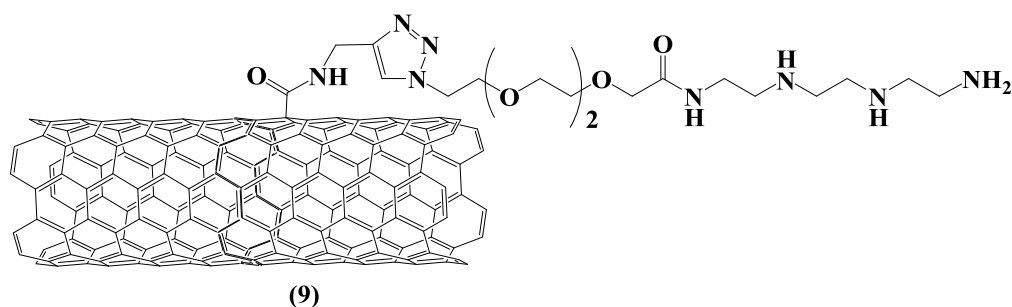
2.3.8 Functionalization of SWCNTs-Alkyne with compound 5 (8)



Solubilized L-ascorbic acid sodium salt (5 mg, 0.02 mmol) and anhydrous CuSO_4 (12 mg, 0.07 mmol) in 5 ml of distilled water. The solution was added to a sonicated mixture of alkyne SWCNTs (6) (30 mg) and compound (5) (100 mg, 0.15 mmol) which was dissolved in 5 ml of DCM, and the reaction was stirred overnight. Added 30 ml Methanol to reaction, then sonicated for 15 min then was filtered, product was washed with (2 x

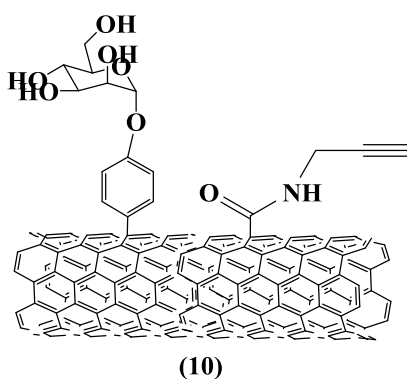
30 ml) MeOH, and (2 x 30 ml) ether. Black powder was dried by vacuum. Then resulting black product was collected and weighed to obtain *f*-SWCNTs 9 (33 mg).

2.3.9 Synthesis of *f*-SWCNTs. (9)



f-SWCNTs (8) (30 mg) was solubilized in 5 ml of DCM and sonicated for 10 min, TFA (4 ml) was added and the reaction was stirred overnight. 30 ml of methanol was added then sonicated and filtered by vacuum. Washing steps were repeated with (2 x 30 ml) MeOH, and (2 x 30 ml) ether to obtain black powder (23 mg).

2.3.10 Functionalization of SWCNTs-Alkyne with compound 7 (10)

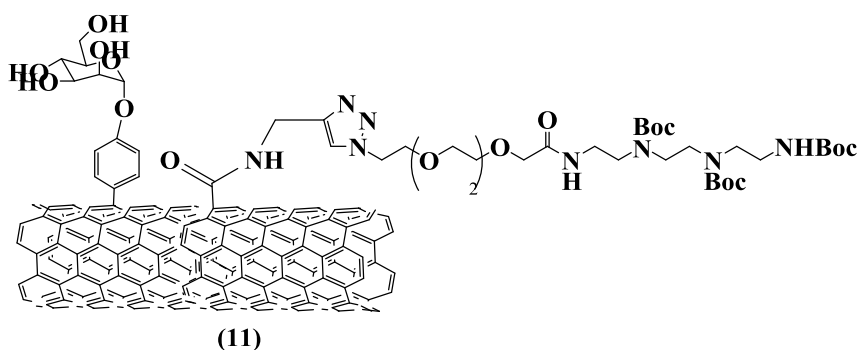


Compound 7 (84 mg, 0.40 mmol) and SWCNTs-alkyne 6 (30 mg) dispersed in *o*-DCB:DMF (2:1, 25 ml) under vacuum and argon. The reaction was sonicated for 30 min under argon bubbling, iso-amyl nitrite

(350 μ l) was added drop by drop to the reaction. The reaction was stirred at 65°C for 24hr under argon. The product was filtered under vacuum, washed with MeOH, acetone and ether to get 55 mg of black powder

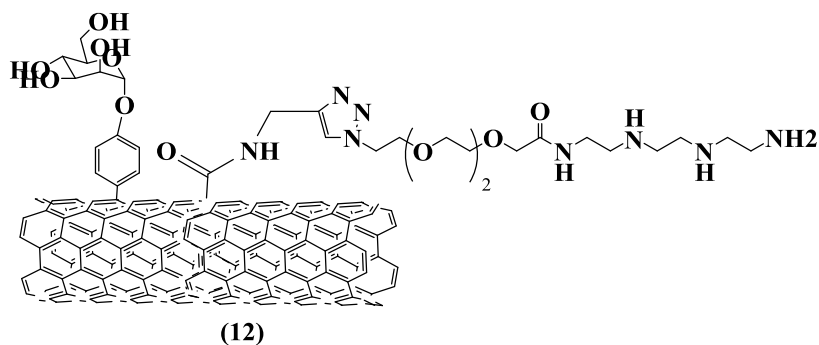
IR: 3645.38, 2917.15, 1562.01 cm^{-1}

2.3.11 Functionalization of *f*-SWCNTs (10) with compound 5 (11)



Compound (11) was synthesized as compound (8).

2.3.12 Deprotection of *f*-SWCNTs 11 (12)



Compound (12) was synthesized as compound (9).

2.3.13 The Quantitative Kaiser Test protocol [for free NH₂ loading determination].

The experiment was done in according to the literature. The result was expressed as mmole of amino groups per gram of SWCNTs [99]. (1.1 mg) was weighted in a small tube. Phenol solution (75 μl), pyridine solution (100 μl) and ninhydrin solution (75 μl) were added to the tube. The blank was prepared exactly with the same quantities of solvents but without the functionalized SWCNTs .The resulting dispersion was sonicated for 5 min. and heated for 10 minutes at 120 °C. The suspension was cooled and diluted with 60% ethanol (1ml) and filtered by glass dropper. The tube was washed with 60% ethanol (2 x 0.5 ml). After that, the filtrate was analyzed by UV spectroscopy at 570 which indicates the amount of free amine functionalized on the CNTs surface using this equation:

$$\text{NH}_2 \text{ Loading (mmol/g)} = \frac{[\text{Abs}_{\text{sample}} - \text{Abs}_{\text{blank}}] \times \text{dilution (mL)} \times 10^3}{\text{Extinction coefficient} \times \text{sample weight (mg)}}$$

2.3.14 Non-covalent functionalization of Dox (13, 14)

1 mg of compound 9 and 12 was added to 1 ml of carbonate buffer and sonicated for 10 min, then 1 mg Dox was mixed with the solution and sonicated for 20 min, then the mixture was incubated for 24 hours at room temperature. After that, the mixture was sonicated for 30 min. and centrifuged at 15000 rpm for 15 min, then the supernatant was removed, and the functionalized SWCNTS were freeze dried. Carbonate buffer was

prepared freshly from 1ml of 0.1M sodium carbonate (10.599g in 1L) and 9ml of 0.1M sodium bicarbonate (8.4g in 1L) at 20 °C and pH 9.16.

2.4 In vitro drug release

2.4.1 Calibration curve of Doxorubicin HCl using spectrophotometry

A calibration curve of Doxorubicin HCl was prepared at λ_{\max} 485 nm using a serial dilutions (0.05, 0.04, 0.03, 0.02 and 0.01 mg/ml) of Doxorubicin (5 mg/5 ml) in distilled water. The calibration curve was constructed by plotting absorbance vs. concentration to determine the quantity of the loaded doxorubicin on the surface of the SWCNTs.

2.4.2 Calibration curve of mannose using spectrophotometry

A calibration curve of mannose was prepared at λ_{\max} 620 nm using a serial dilutions (0.05, 0.04, 0.03, 0.02 and 0.01 mg/ml) of mannose (1 mg/ml) in distilled water according to anthrone method.

2.4.2.1 Anthrone method

0.5ml from a serial dilutions (0.05, 0.04, 0.03, 0.02 and 0.01 mg/ml) of mannose (1 mg/ml) in distilled water was added to 1 ml of (0.2% anthrone in sulfuric acid) at 0°C. After that, the mixture was incubated for 10 min at 100° C. Then, the mixture was transferred to ice until reach the room temperature. After that, the absorbance was measured at $\lambda_{\max} = 620$ nm [100, 101].

2.5 Anticancer activity

2.5.1 Cell line

The cytotoxicity of the test compounds was investigated on human colorectal adenocarcinoma cell line (Caco2) cells and breast adenocarcinoma cell line (MCF-7).

2.5.2 Cell culture

The cells were cultured in T-175 cell culture flasks supplemented with cell culture growth medium (CGM) composed of RPMI basal medium supplemented with L-glutamine (1%), FBS (10%), and penicillin/streptomycin (1%). The cells were kept in standard cell culture incubator at 5% CO₂, 37°C and 99% humidity.

For sub-culturing, the medium was suctioned and washed with excess of Ca²⁺-free PBS. After that, the cells were incubated with 0.025% trypsin for up to 5 min in the cell culture incubator until sufficient cells detached from the flask. Then trypsin was inactivated by CGM, the cell suspension was collected, and the viable cell count was determined using trypan blue stain before adjusting the cell concentration to 50.000 cell/ml. Finally the cells were seeded in 96-well plate as 5000 cell/well. The cells were left to adhere and accommodate overnight before running any test.

2.5.3 Cytotoxicity test

A concentration-dependent cytotoxicity experiment was performed for the test substances for equivalent concentrations of Dox (0.0, 0.5, 1.0, 2.0 and 4.0 $\mu\text{g/ml}$) under 7.4 pH condition, where 100 μl of the test medium was used per well. After overnight incubation with the test conditions, 10 μl of MTS reagent was added to the whole wells and incubated for 1 hr in cell culture incubator. After that the absorbance was measured at 490 nm by a plate reader.

2.5.4 Mannose receptor selectivity test

Cells were cultured in 96 well plate, as described above, were incubated for 30 min with CGM supplemented with different concentrations of mannose (1500 μM , 1000 μM , 500 μM , 0 μM) in a cell culture incubator. After that, the medium was exchanged for CGM containing, in addition to mannose, different concentrations of the test substances at pH 7.4. The cells were incubated for 24hr. After that, MTS test was performed as explained above.

2.5.5 Statistical Analysis

Statistical analysis was performed by using GraphPad Prism version 6.01 for Windows, GraphPad Software, La Jolla California USA, www.graphpad.com, version 6.01. The data was presented as mean \pm standard error mean, and Student t-test was used to compare the means. The difference was considered significant when p value was ≤ 0.05 .

2.6 Isolation of RNA

According to the manufacturer procedure, 3×10^6 cells (Caco2 or MCF-7) were seeded per well of 6-well plates. The growth medium was removed, then 400 μL of Triazol reagent was added per well and the plate was incubated at 37°C over a period of 5 minutes in order to permit complete lysis of the cells and complete dissociation of the nucleoproteins complexes. The lysate was transferred into DNase/RNase free tubes, each tube then received 80 μL of chloroform, and were incubated for 2–3 min. at 37°C . Afterwards the samples were centrifuged for 15 min. at $12,000 \times g$ at 4°C . As a result, the mixture was separated into two layer, a lower red phenol-chloroform (organic) layer with interphase, and an upper colorless aqueous layer. The aqueous layers containing the RNA (upper layer) were carefully transferred to new tubes, and 200 μL /tube of iso-propanol was added. Then the tubes were incubated for 10 minutes at 37°C , followed by centrifugation at $12,000 \times g$ at 4°C for 10 minutes, which allowed RNA precipitation as a white pellets at the bottom of the tubes. The supernatant was removed then the pellet was re-suspended in 400 μL of 75% ethanol, then the samples were vortexed briefly, centrifuged at $7500 \times g$ at 4°C for 5 minutes, and the supernatant was again discarded, then the RNA white pellet was left to dry for 5–10 minutes at 37°C . The RNA pellets were re-suspended and dissolved in 50 μL of RNase-free water with warming to 60°C for 10–15 minutes. Finally RNA concentration was determined by measuring the absorbance at 260nm (A_{260}) in a spectrophotometer

2.6.1 Gel electrophoresis experiments

2.6.1.1 Composition of FA gel buffers

2.6.1.1.1 10x FA gel buffer

MOPS (41.46 g), sodium acetate (6.8 g), and EDTA (2.9 g) were mixed and completed with distilled water up to 1 L, pH was adjusted to 7.0 by using NaOH

2.6.1.1.2 1x FA gel running buffer

10x FA gel buffer (100 ml), was mixed with 37% (12.3 M) formaldehyde (20 ml) and completed with RNase-free water to 880 ml.

2.6.1.1.3 5x RNA loading buffer

16 μ l of saturated aqueous bromophenol blue solution, 80 μ l of 500 mM EDTA (EDTA solution adjusted previously with NaOH to pH 8.0), 720 μ l of 37% (12.3 M) formaldehyde, 2 ml 100% glycerol, 3.084ml formamide, 4 ml of 10 x FA gel buffer were mixed and completed to 10 ml with RNase-free water.

2.6.1.2 Formaldehyde Agarose gel

1.2 g agarose was added to 10 ml of 10x FA gel buffer and was completed with RNase-free water to 100 ml. To melt agarose the mixture was heated by microwave and then was left to cool to 65°C. After that 1.8 ml of 37% formaldehyde and 1 μ l (10 mg/ml) ethidium bromide were added and the warm solution was poured in gel cassette and appropriate combs were

inserted to create wells. After polymerization for 30 min, the agarose gel was submerged in 1x FA gel running buffer in order to equilibrate for at least 30 min.

2.6.1.3 RNA sample preparation, loading and running

RNA sample was mixed with 5x RNA loading buffer in a ratio 1:4, then the sample was incubated for 3–5 min at 65°C, then chilled on ice, and loaded onto the equilibrated FA gel. The electrophoresis was run at 70 V for 1 hr.

2.7 Verification of the primers

The QIAGEN OneStep RT-PCR Kit was used for RNA reverse transcription and PCR amplification for the RNA of β -actin, β -catenin and WNT by using specific primers for these genes. A master mix of PCR reaction was prepared for each primer pair according to manufacturer procedure as shown in the following table:

Table 2. 1 : Components for one-step RT-PCR Reaction

Component	Volume (μ L)
5x QIAGEN OneStep RT-PCR Buffer	1
Template RNA	0.5
dNTP Mix	5
RNase-free water (provided)	14.5
Primer A (10 μ M)	1.5
Primer B (10 μ M)	1.5
QIAGEN OneStep RT-PCR Enzyme Mix	1
Total volume	25

Then the reaction tubes was put in PCR machine and the following protocol was applied.

Table 2. 2 : Thermal cycler conditions for β -actin

β -actin	No. of cycle
50 °C/30 min	
95°C/15 min	
94°C/40 sec	40 cycle
55 °C/40 sec	
72 °C/60 sec	
72 °C/10 min	Final extension

Table 2. 3 : Thermal cycler conditions for β -catenin

β -catenin	No. of cycle
50 °C/30 min	
95°C/15 min	
94°C/40 sec	40 cycle
50 °C/40 sec	
72 °C/60 sec	
72 °C/10 min	Final extension

Table 2. 4: Thermal cycler conditions for WNT

WNT	No. of cycle
50 °C/30 min	
95°C/15 min	
94°C/40 sec	40 cycle
50 °C/40 sec	
72 °C/60 sec	
72 °C/10 min	Final extension

2.8 Loading PCR samples and running Gel electrophoresis

0.5 g agarose and 50 ml 1X TAE buffer were dissolved to prepare 1% agarose gel. The mixture was heated with intermittent stirring until the powder was completely dissolved in the buffer. After that one drop of 1mg/ml of (EtBr) was add to the solution during cooling down at room temperature before the solution was casted in gels cassettes.

2.9 Knockdown and reverse transfection of β -catenin gene

2.9.1 Cell culture

Caco2, and MCF-7 suspension was prepared in serum free & antibiotic-free medium as mention previously. After trypsin inactivation with serum-containing medium, the cells were collected and the living cells were counted, then they were spinned down at 150 g for 7 min, the supernatant was completely removed, and the cells were re-suspended in serum free & antibiotic-free medium so that the cell concentration is 300,000 cell/ml (based on the cell count).

2.9.2 Transfection Complex preparation

9 μ L of Lipofectamine RNAiMAX Reagent was diluted with 150 μ L medium (containing no serum, no antibiotic). In parallel 10 μ L siRNA (10 μ M) was diluted with 150 μ L medium (no serum, no antibiotic). Then the diluted siRNA was added to the diluted Lipofectamine RNAiMAX (1:1 ratio) and then the mixture was incubated at room temperature for 20 min. The transfection mixture (300 μ L) was transferred to a well of 6-well plate, then 2 ml of cell suspension (300,000 cell/ml) were added to the well, after that the plate was incubated for 4 hr. After that 250 μ l serum, 25 μ l antibiotic stock and 1 ml complete medium were added, and incubated overnight.

2.9.3 Verification Step (Isolate RNA and perform PCR)

Procedure of isolation and PCR run were performed as explained above.

2.10 Complexion of *f*-SWCNT (12) with siRNA

f-SWCNT was mixed with siRNA at different N/P ratios; 1.25:1, 2.5:1, 5:1, 7.5:1 and 10:1 (N/P ratio defined as the molar ratio of nitrogen in *f*-SWCNT to phosphate group in the siRNA). In order to guarantee the consistency of the signal intensity on the gel, the amount of the siRNA was fixed 50 pmole while the amount of *f*-SWCNT was increased according to the intended N/P ratio. The mixtures *f*-SWCNT and siRNA were mixed vigorously and were then incubation for 45 min at 37°C.

2.11 Loading Samples and Running on Agarose Gel

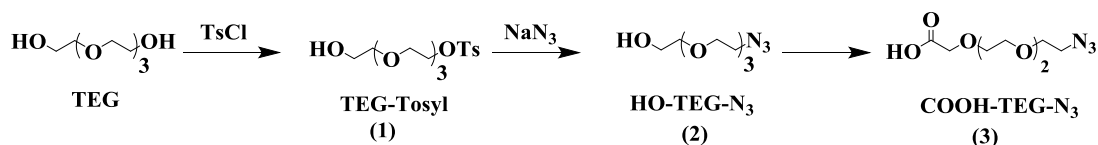
siRNA-SWCNT complex samples with different N/P ratios were prepared as explained above. DNA loading buffer was added to the samples and were loaded to 4% agarose gel submerged in TAE buffer. The electrophoresis was run at a voltage of 110 volte for 30 min. The gel was visualized by a UV PhotoDoc-It imaging system.

Chapter Three

Results and Discussion

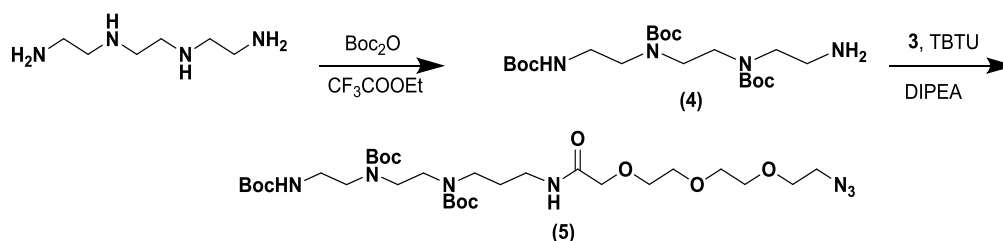
3.1 Synthesis and functionalization of SWCNTs

In this thesis, we aim to achieve triple functionalization of the SWCNTs in order to selectively target the cancer cells and to have a synergistic activity to kill the cancer cells more efficiently. Moreover, the approach used to improve the water dispersibility of the SWCNTs as they have low water solubility. Therefore, the Dox (the anticancer drug) was loaded on the surface of the SWCNTs non covalently through π - π stacking, mannose is the targeting agent was attached to the SWCNTs covalently through diazonium reaction. Finally, the silencing RNA (siRNA) of the β -catenin protein that is considered the anti-apoptotic protein was loaded through electrostatic interaction with a synthesized multi amine spacer. Therefore, in the following section we introduce the synthesis of the multi amine spacer and the process of the functionalization of SWCNTs. First of all, we used a derivative of tetraethylene glycol as a linker between the SWCNTs and the multi amine spacer. A derivative of tetraethylene glycol (TEG) was synthesized using several steps started with the reaction of OH group of TEG with tosyl group to get compound **(1)**. After that, the tosyl group was replaced with azide group through the reaction of **(1)** with sodium azide in EtOH to get TEG-N₃ **(2)**. Therefore, compound **(2)** was oxidized by Jones's reagent to get compound **(3)** as shown in **Scheme 5**.



Scheme 5: Synthesis of linker 3 (COOH-TEG-N₃).

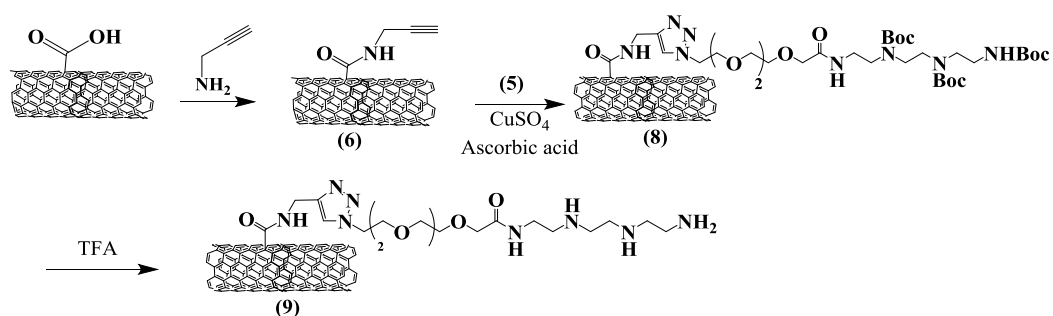
Once the linker 3 was synthesized successfully which is an important linker in order to increase the water dispersibility and the biocompatibility of the functionalized SWCNTs. Therefore, The tetraamine spacer was attached to compound (3). Beginning with a selective protection of triethylene tetraamine with Boc groups to get compound (4). The Boc protected tetra amine spacer was reacted with compound (3) through amidation reaction using TBTU as coupling agent and DIPEA as base to get compound (5) as shown in **Scheme 6**.



Scheme 6: Synthesis of compound (5).

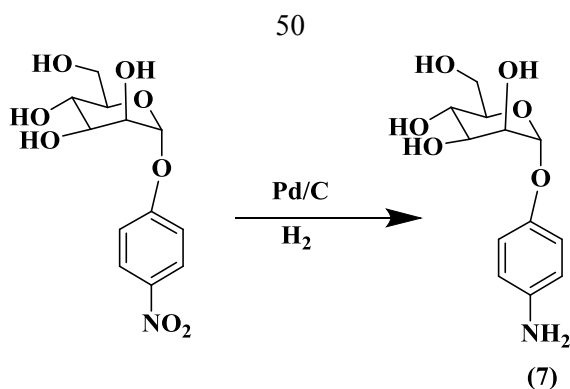
The next step is to attach compound (5) to the SWCNTs. So, the carboxylated-SWCNTs were functionalized covalently with propargylamine through amidation reaction to get terminal alkyne group SWCNTs (6). After that, the click reaction was performed between compound (5) and *f*-SWCNTs (6) using copper sulfate and ascorbic acid in DCM:H₂O (1:1) to get *f*-SWCNTs (8). After that, the Boc group was removed under acidic conditions using TFA to get the SWCNTs have the

tetramine spacer (**9**) as shown in **Scheme 7**. The loaded amine value was determined by Kaiser test. The amine loading was 0.0347 mmol /gram of *f*-SWCNTs (**9**), **Scheme 7**. This functionalized SWCNTs was used as a control for the delivery of only the siRNA as a control compound.



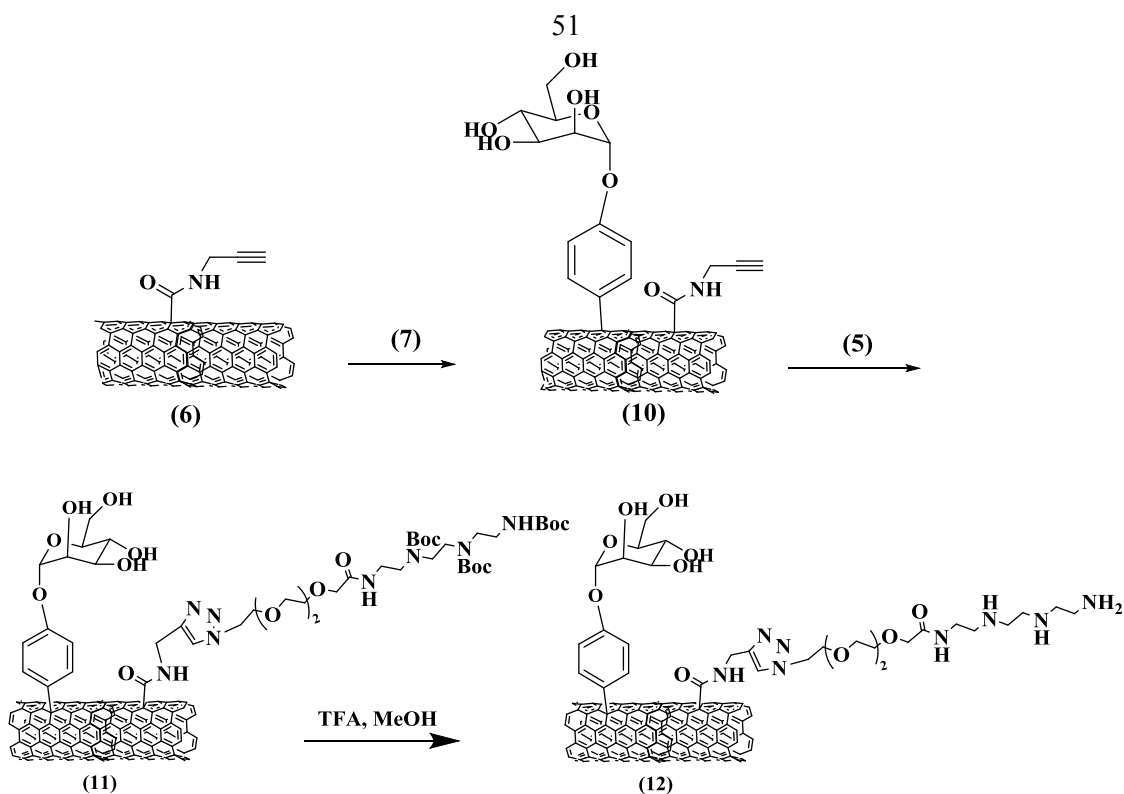
Scheme 7: functionalization of Alkyne-SWCNTs with tetramine spacer.

After the monofunctionalization of SWCNTs with the tetramine spacer, we aimed to dual functionalization of the SWCNTs with tetramine spacer and a targeting agent (mannose) in order to specifically targeting the cancer cells. As we discussed in the introduction, some cancer cell lines overexpressed mannose receptors on their surface especially hepatic cancer and breast cancer. Therefore and to achieve this aim, 4-nitrophenyl α -D-mannopyranoside was reduced using palladium over carbon as a catalyst in the presence of hydrogen in order to obtain 4-aminophenyl α -D-mannopyranoside (**7**), as shown in **Scheme 8**, that can be bind to SWCNTs through diazonium reaction (Tour reaction).



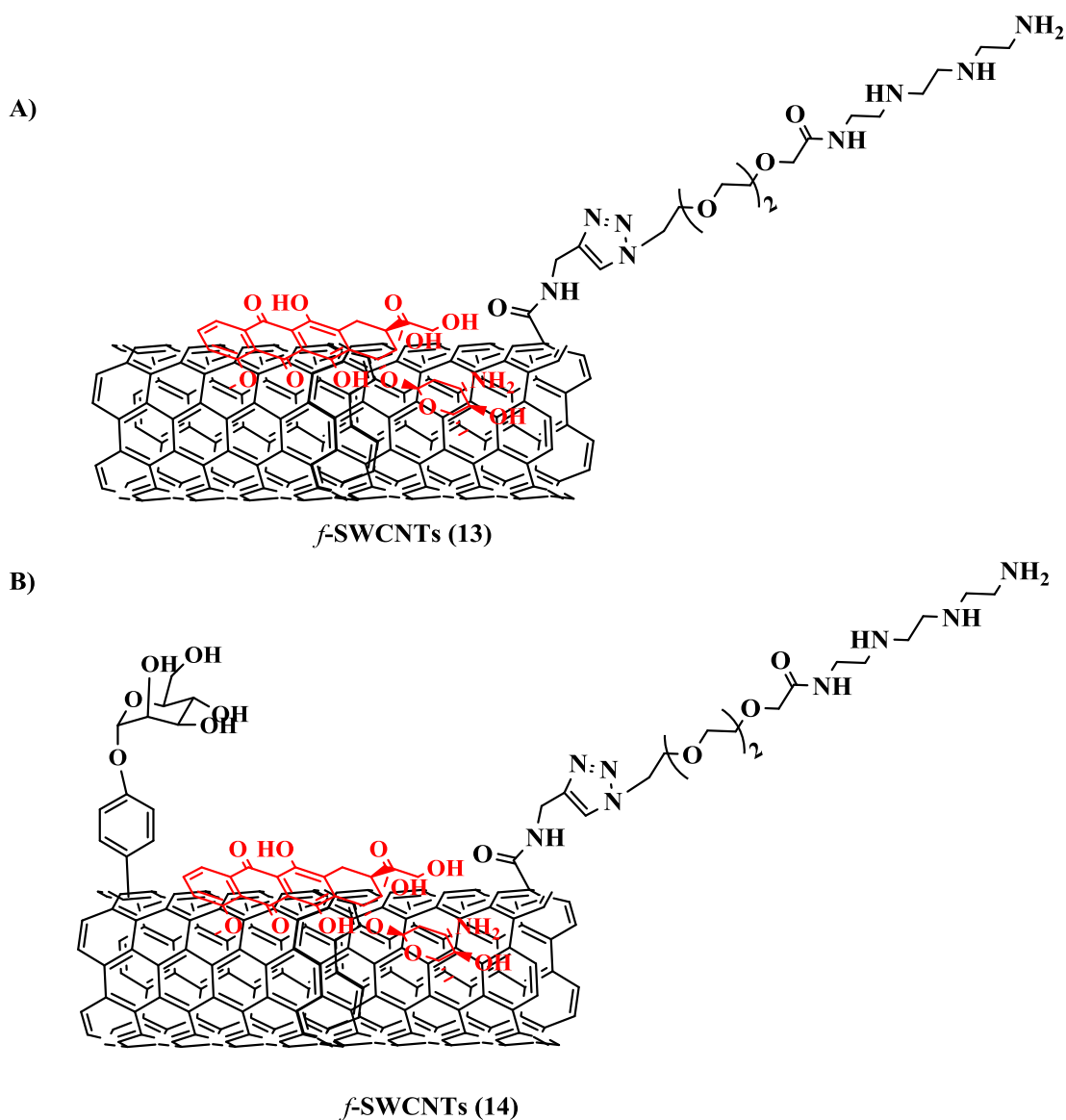
Scheme 8: Synthesis of 4-aminophenyl α -D-mannopyranoside

The reaction of compound (7) with *f*-SWCNTs (6) was conducted through Tour reaction by using iso-amyl nitrite as catalyst, which dissolved in *o*-DCB and DMF to obtain compound (10). After that, the *f*-SWCNTs (10) were reacted with compound (5) through click reaction by using anhydrous CuSO₄ and ascorbic acid as catalysts which dissolved in DCM and water to obtain the *f*-SWCNTs (11). After that, the Boc group was removed under acidic conditions using TFA to get the functionalized SWCNTs (12) as shown in *Scheme 9*. The loaded amine value was determined by Kaiser test. The amine loading was 0.0352 mmol /gram of *f*-SWCNTs (12).



Scheme 9: Dual functionalization of SWCNTs to obtain the *f*-SWCNTs (12)

Finally and in order to functionalize compounds **9** and **12** with Doxorubicin, they were incubated with a solution of the Dox in bicarbonate buffer in order to be adsorbed noncovalently on the surface of the *f*-SWCNTs (**9**) and *f*-SWCNTs (**12**) to obtain *f*-SWCNTs **13** and **14**, respectively as shown in *Scheme 10*. *f*-SWCNTs (**13**) was prepared in order to test the targeting agent importance. *f*-SWCNTs (**14**) will contain the tetramine spacer, targeting agent and the Doxorubicin.



Scheme 10: Non-Covalent functionalization of *f*-SWCNTs (9) and (12) with Doxorubicin.

3.2 Characterization of Di-*f*-SWCNTs and Tri-*f*-mannose-SWCNTs

3.2.1 TEM images of the functionalized SWCNTs

The functionalized SWCNTs were characterized by TEM in order to study the morphology of the carbon nanotubes. The pristine carbon nanotubes are found as a bundles of nanotubes due to the Van der Waals interactions between the nanotubes, **Figure 3. 1A**. However, upon the functionalization

the nanotubes become separated and can be found as single nanotubes due to the repulsion between them as shown in **Figure 3. 1B**.

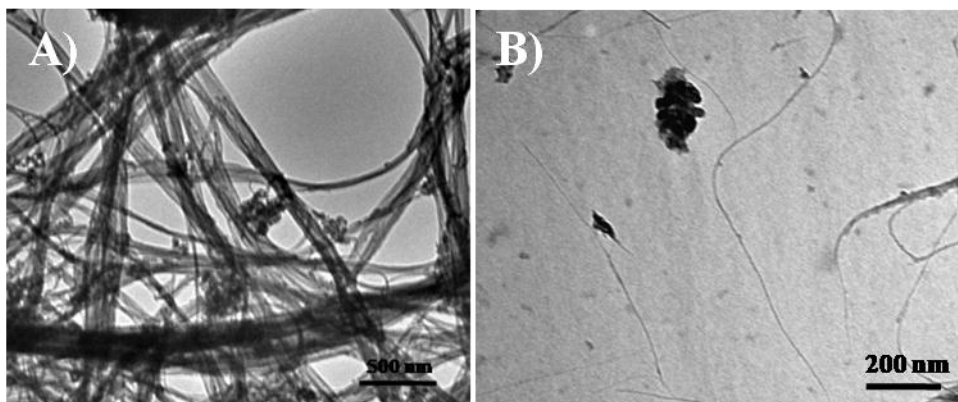


Figure 3. 1 : TEM images of A) pristine SWCNTs; B) f-SWCNTs **14**.

3.2.2 UV-vis spectrophotometry

3.2.2.1 Calibration curve of Doxorubicin

The loaded amount of Dox was measured by spectrophotometry. A calibration curve of Dox has been constructed at $\lambda_{max} = 485$ nm with a R_2 0.996 as shown in **Figure 3. 2**. The loaded amount of Dox on SWCNTs was about 173.96 $\mu\text{g}/\text{mg}$ of Di-*f*-SWCNTs (**13**) and 219 $\mu\text{g}/\text{mg}$ of Tri-*f*-SWCNTs (**14**).

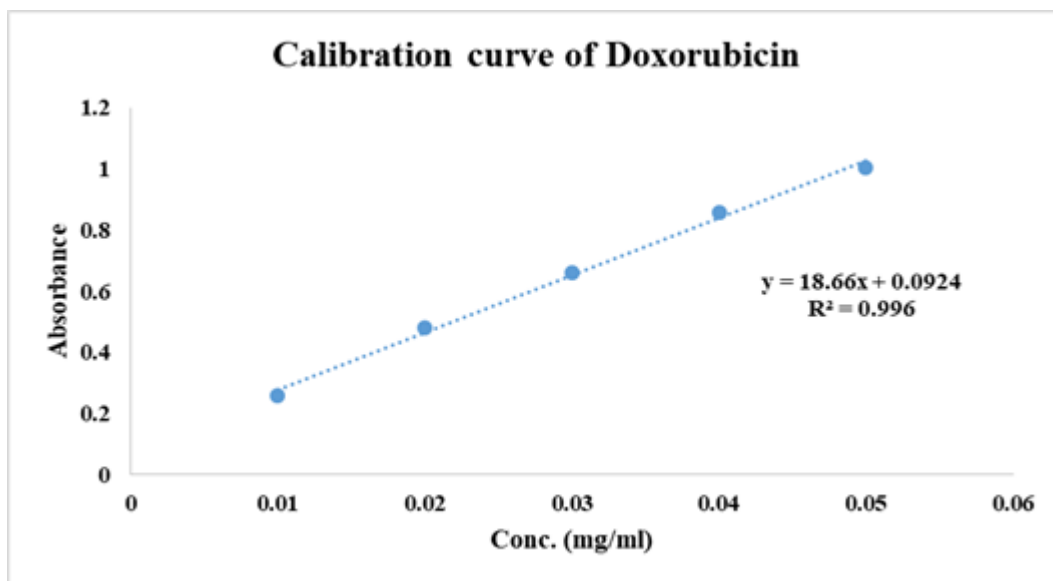


Figure 3. 2: Calibration curve of Dox in distilled water at $\lambda_{max} = 485\text{nm}$.

3.2.2.2 Calibration curve of Mannose

The loaded amount of mannose was measured by spectrophotometry using anthrone method [100, 101]. A calibration curve of mannose has been done at $\lambda_{max} = 620 \text{ nm}$ and R_2 was 0.9966, **Figure 3. 3**. The loaded amount of mannose on SWCNTs was about $79.66 \mu\text{g}/\text{mg}$ of Tri-*f*-SWCNTs (14).

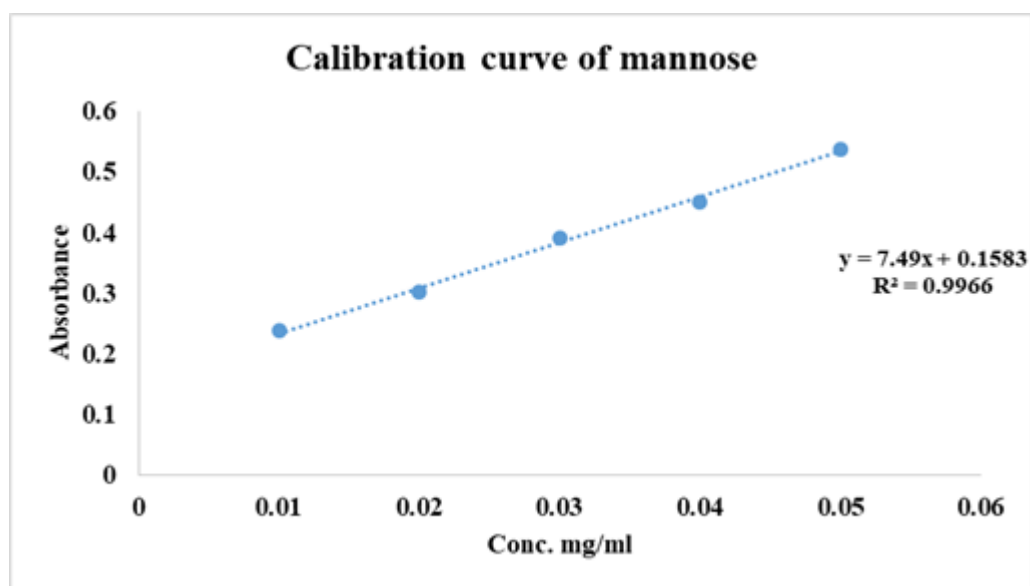


Figure 3. 3: Calibration curve of Mannose in distilled water at $\lambda_{max}=620\text{nm}$.

3.2.3 Thermogravimetric analysis (TGA)

A thermogravimetric analysis was conducted in order to quantify the total amount of the functionalization on the surface of the single walled carbon nanotubes in final compounds (**14**). It is well known that the pristine SWCNTs are thermostable until 600 °C and will not be degraded upon heating as shown in *Figure 3. 4* the black dots. After the organic triple functionalization of SWCNTs, the heating will degrade the organic compounds and there will be a loss of the weight of the SWCNTs as shown in *Figure 3. 4* the red dots. As shown in the figure, there is a 77.5% of functionalization which is considered a high percentage of functionalization that confirms the successful triple functionalization of SWCNTs.

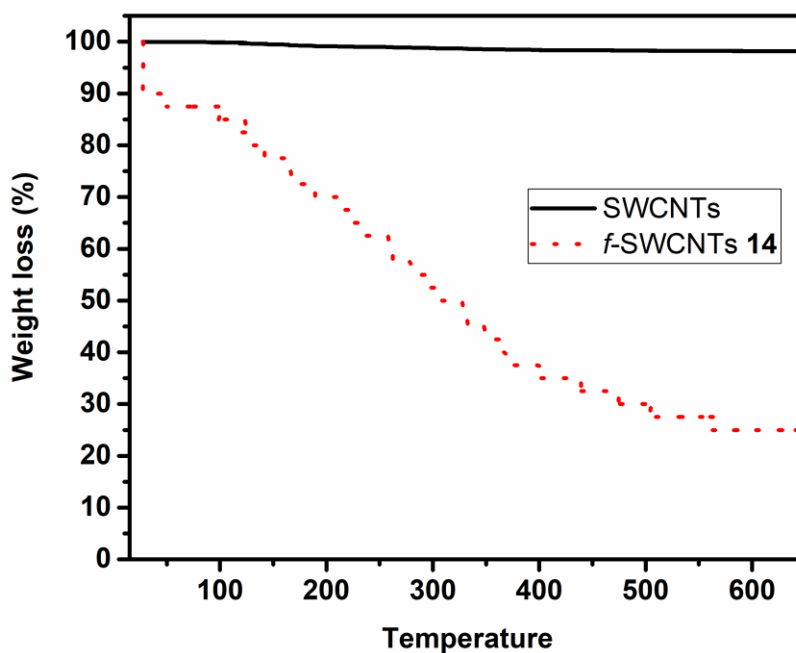


Figure 3. 4 :Thermogravimetric analysis of pristine SWCNTs (black dots) and f-SWCNTs **14** (red dots).

3.2.4 Zeta potential analysis

Zeta potential measurement was used to determine the stability of the suspension and provide a measure of the magnitude and sign of the effective surface charge associated with the layer around the functionalized SWCNTs.

Therefore, the zeta potential obtained for the Di-*f*-SWCNTs was +28 mV and for the tri-*f*-SWCNTs was +47 mV, which indicates the positive charge surrounding the surface of the SWCNT due to the tetramine functionalization, the highly positive charge of zeta potential on the surface of CNTs leads to repulsion with SWCNT and according to several studies, the increasing of zeta potential values more than +20 will confirm the stability and dispersibility of the functionalized SWCNTs[102].

3.3 Cytotoxic activity

3.4.1 Concentration and pH-dependent effect on the cytotoxicity of the test compounds

Caco2 and MCF-7 cell lines were used to investigate the cytotoxic efficacy of Di-*f*-SWCNTs which contains tetraamine linker and Dox, and Tri-*f*-SWCNTs which contains tetraamine linker, mannose, and Dox by using MTS assay. Free Dox and blank CGM were used as controls. Concentration-dependent and pH dependent studies were performed in parallel. For Caco2 cells, the cytotoxicity of Dox was comparable to that of the corresponding equivalent Dox concentrations loaded on SWCNT and at

corresponding pH (**Figure 3. 5 A-C**). However, Dox and Tri-*f*-SWCNTs showed pH-dependent improvement in cytotoxicity at a concentration of 4mcg/ml (**Figure 3. 5D**).

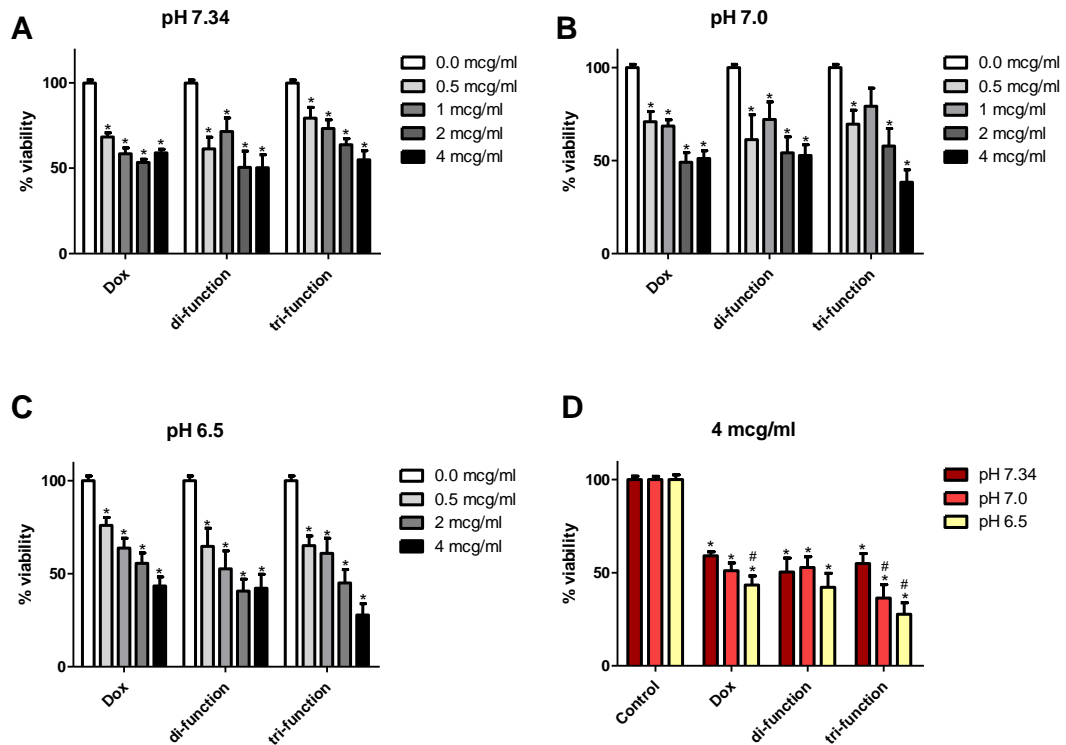


Figure 3. 5: Concentration-dependent effect on Caco2 cell viability at different pH values: A) at pH = 7.34, B) at pH = 7.0, C) at pH = 6.5. D) pH dependent effect at a concentration equivalent to 4 mcg/ml Dox. (n=6, *p<0.05, compared to the negative control 0.0 mcg/ml, # p<0.05, compared to the same species concentration at pH = 7.34).

On the other hand, for MCF-7 cells Dox had low cytotoxicity at pH 7.34 and 7.0, even at 4 mcg/ml, as evident by cell viability readings of around 80%. However, the cytotoxicity significantly improved at pH 6.5, where it showed a clear concentration-dependent effect. Interestingly, when Dox was loaded on SWCNT, whether as Di- or Tri-*f*-SWCNT, it could induce

greater cytotoxicity at all tested pHs, with the highest effect observed by 4 mcg/ml Tri-*f*-SWCNT at pH 6.5, which suggests that the presence of loaded mannose could increase the uptake of the complex (**Figure 3. 6 A-C**). By investigating the pH-dependent effect at 4 mcg/ml Dox concentration, it was found that the acidic pH improved only slightly the effect of free Dox, but it showed no significant change in the activity of the loaded Dox on SWCNT (**Figure 3. 6D**), which might be an advantage for targeting cancer tumor tissues with different pH conditions, as Dox can be released from the complex at any pH even in acidic cancer medium, while maintaining the same level of cytotoxicity.

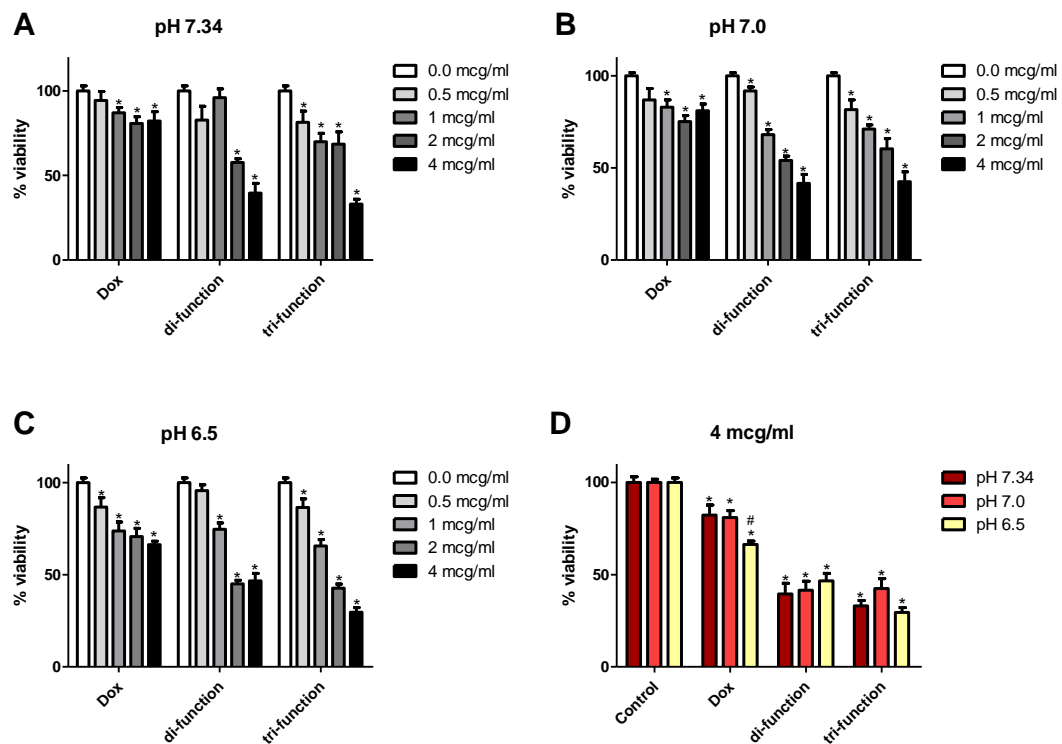


Figure 3. 6 : Concentration-dependent effect on MCF7 cell viability at different pH values: A) at pH = 7.34, B) at pH = 7.0, C) at pH = 6.5. D) pH dependent effect at a concentration equivalent to 4 mcg/ml Dox. (n=6, *p<0.05, compared to the negative control 0.0 mcg/ml, # p<0.05, compared to the same species concentration at pH = 7.34).

3.4.2 Loading mannose on SWCNT and its effect of the cytotoxicity of the test compounds

The loading of mannose on SWCNT could increase the cytotoxicity of the complex as shown in **Figure 3. 5 D** and **Figure 3. 6 D**. We hypothesized that mannose might facilitate receptor-mediated endocytosis. In order to test this hypothesis the cells were incubated with CGM supplemented by different concentrations of mannose for 30 min (so as to induce mannose receptors down regulation) before the medium was exchanged for CGM with pH adjusted to 6.5 and supplemented with 4 mcg/ml of either of the test substances. After about 24 hr, MTS assay was performed. As shown in **Figure 3. 7** and **Figure 3. 8**, the pre-incubation with any of the tested concentrations of mannose reduced the cytotoxicity of Dox-mannose-SWCNTs by approximately 96-98% in Caco2 and MCF-7, suggesting that the entry of this complex might be dependent on mannose receptors, which imparts this complex a kind of selectivity for cancer cells that overexpress this type of receptors.

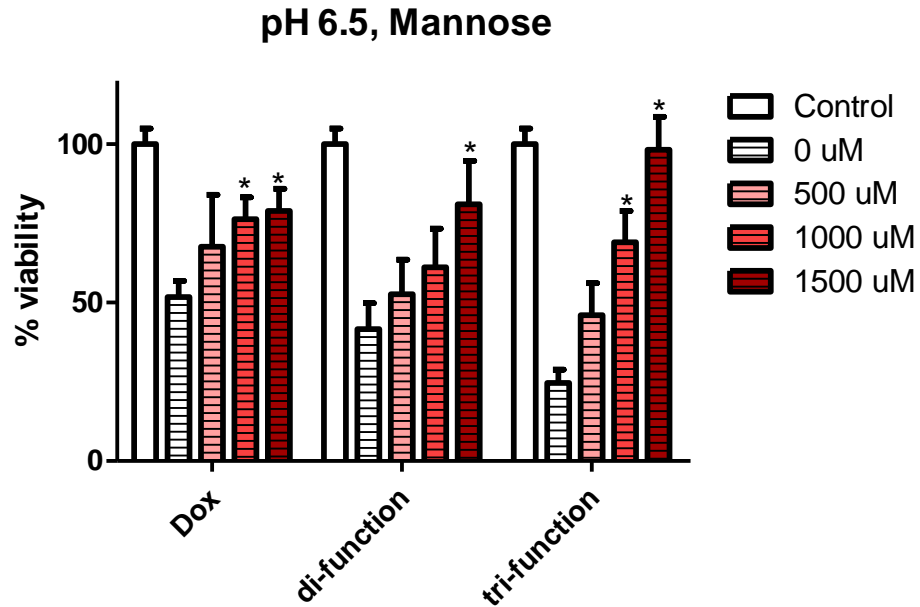


Figure 3. 7: Effect of pre-incubation with mannose on the cytotoxicity of different test substances in Caco2 cell line at a concentration 4 mcg/ml and a pH of 6.5 (n=3, *p<0.05, compared to 0 μ M mannose).

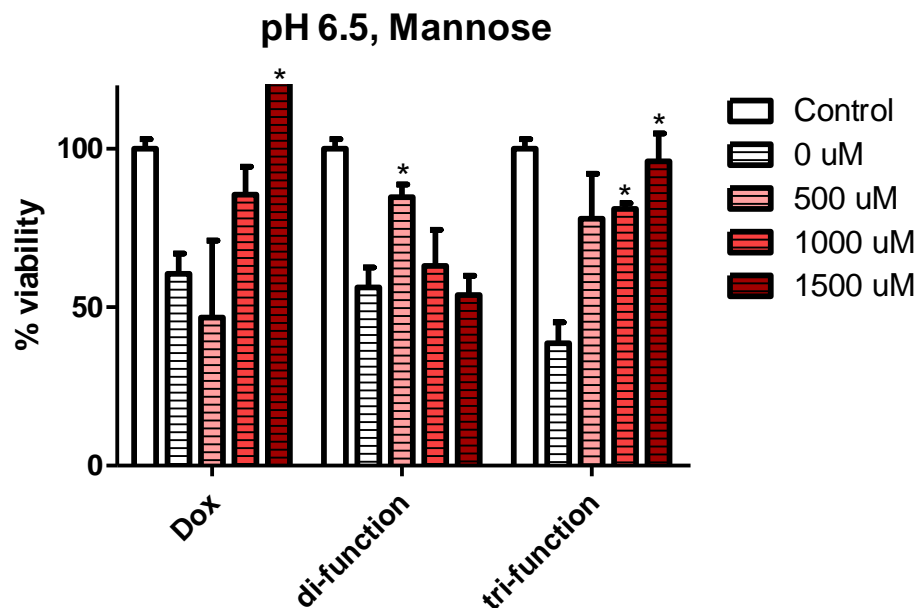


Figure 3. 8 : Effect of pre-incubation with mannose on the cytotoxicity of different test substances in MCF-7 cell line at a concentration 4 mcg/ml and a pH of 6.5 (n=3, *p<0.05, compared to 0 μ M mannose).

3.5 Evaluation of RNA

3.5.1 Quantification of RNA

The concentration of RNA was determined by measuring the sample absorbance at 260 nm in a spectrophotometer. The absorbance readings of RNA which was isolated from Caco2 and MCF-7 cells were 0.256 and 0.068 respectively. From these readings the RNA yields were calculated to be 256 μg and 68 μg respectively.

3.5.2 Integrity of RNA

RNA agarose gel electrophoresis was employed to investigate the integrity of isolated RNA. The integrity was adequate as concluded from the presence of the obvious ribosomal RNA (rRNA) bands with minimal smearing.

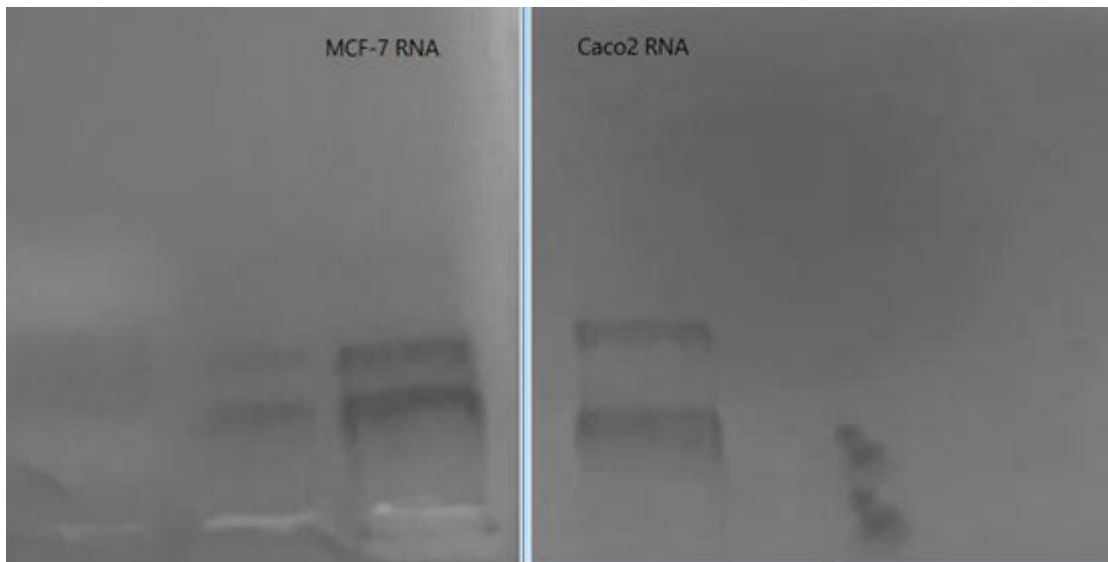


Figure 3. 9: Quality assessment for the isolated RNA by agarose gel electrophoresis.

3.6 Verification of the primers functionality

The products of PCR reactions that included primers for β -catenin, WNT and β -actin were subjected to DNA agarose gel electrophoresis. The gel showed thick bands at the level of around 350 bp (according to the used DNA ladder) for the samples that included primers for β -catenin and β -actin, but not WNT, which indicated that the used primers were able to amplify RNA-derived cDNA segments from β -catenin and β -actin genes. Based on this result, it was decided to knock-down β -catenin while using β -actin as a housekeeping gene.

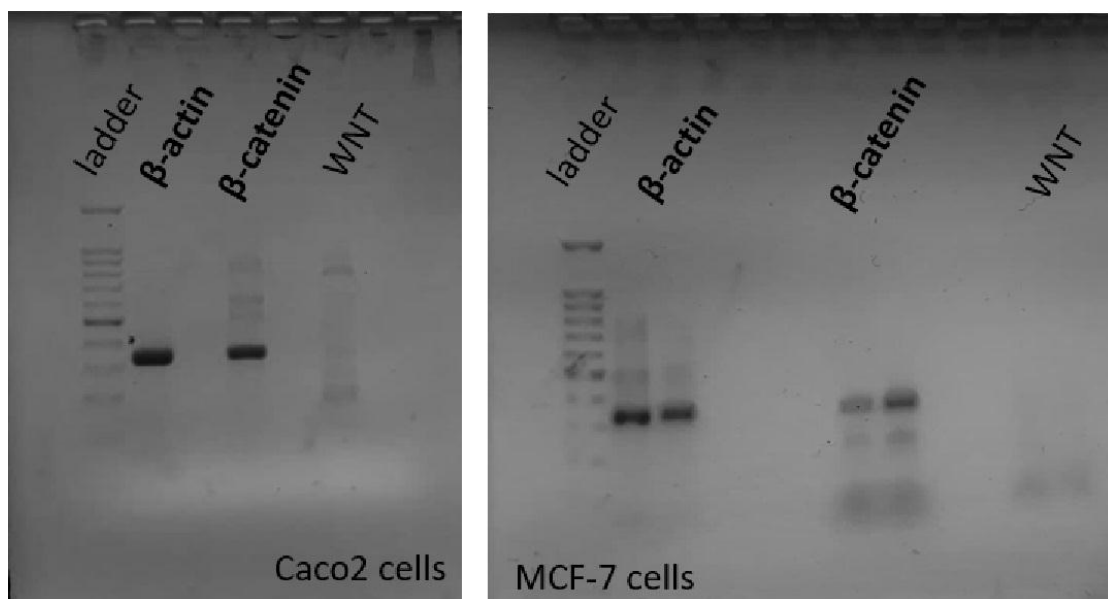


Figure 3. 10 : Figure.3.4: Agarose gel electrophoresis subjected to UV light to verify primers.

3.7 Knockdown of β -catenin

After incubation of siRNA with the cells as explained before, the RNA was extracted, checked for quality and subjected to RT-PCR followed by DNA gel electrophoresis as detailed before in the chapter of methods. The gel

was imaged digitally and the density of the bands was analyzed by ImageJ software. For Caco2 cells, the gel showed a reduction in the density of β -catenin bands by around 20% as compared with the band of the housekeeping gene β -actin. However, the siRNA could not knockdown β -catenin in MCF-7 cells.

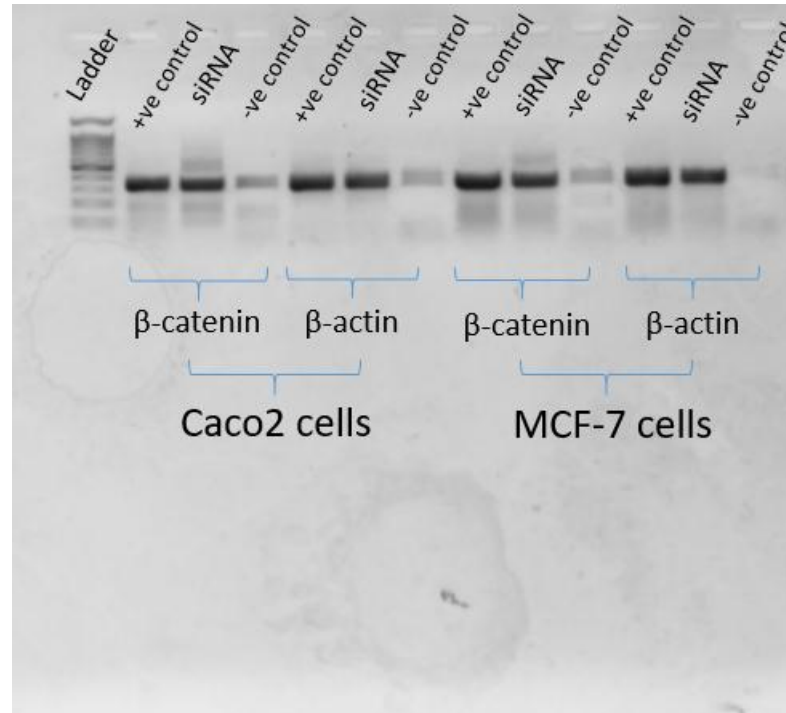


Figure 3. 11 : Agarose gel electrophoresis subjected to UV light to show siRNA transfection of cell lines

3.8 Evaluation of f-SWCNT-siRNA Complex formation

Agarose gel electrophoresis was employed to investigate the formation of *f*-SWCNT-siRNA complex at various N/P ratio (1.25:1, 2.5:1, 5:1, 7.5:1 and 10:1). This would be indicated by a retard of siRNA migration through agarose gel. In the same time siRNA-SWCNT complex formation should be reversible as the siRNA should be released inside the cells to get the chance to interact with mRNA within the cells. As shown in **Figure 3. 12**

the siRNA could completely complexate with *f*-SWCNT at a ratio of all ratios.

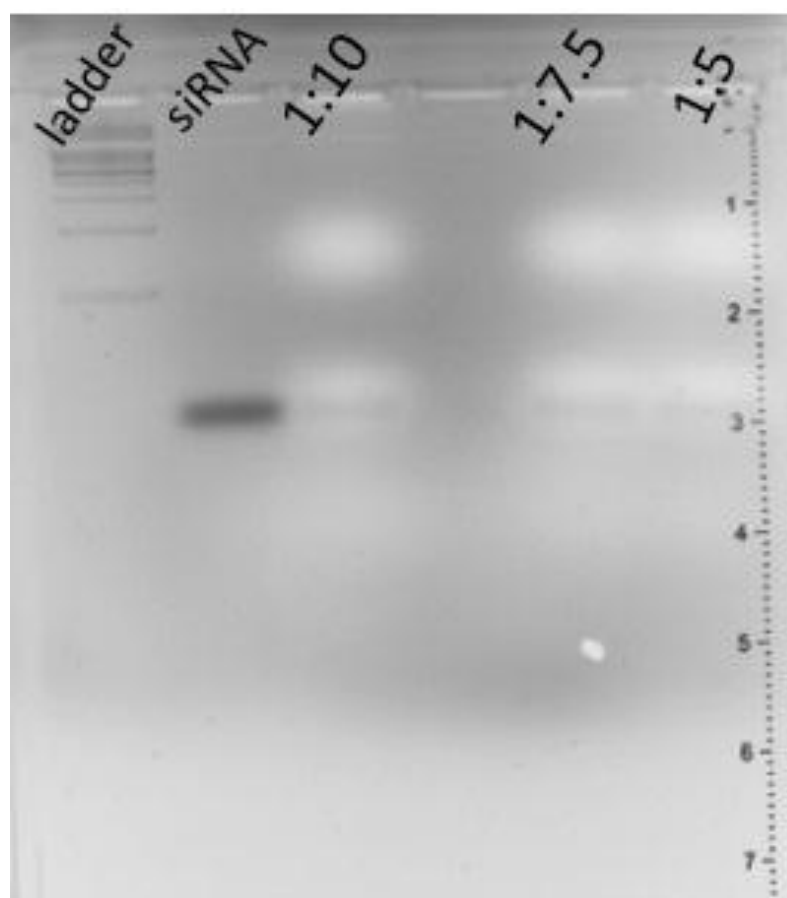


Figure 3. 12 : Agarose gel electrophoresis subjected to UV light to visualize free RNA

Conclusion

The multi functionalization of SWCNTs with tetraamine spacer, targeting agent, mannose, and Dox on the surface of the SWCNTs have successfully been obtained. Moreover tetraamine spacer was included to pair siRNA. The functionalization demonstrated good dispersibility of the f-SWCNTs as confirmed by TEM. The degree of functionalization was 77.5% for compound (14) as confirmed by TGA which is confirmed the high degree of functionalization. The total amine loading was 0.0352 mmol /gram of f-SWCNTs (12), and 0.0347 mmol /gram of f-SWCNTs (9). Referring to the anticancer activity, the MTS proliferation assay showed that it could induce greater cytotoxicity at all tested pHs, with the highest effect observed by 4 mcg/ml Tri-f-SWCNT at pH 6.5. Moreover, the mannose receptor selectivity test result showed that the compound (13) and (14) has mannose receptor selectivity that result to target the cancer cell which express mannose receptor. The integrity of isolated RNA was adequate and the yields for Caco2 and MCF-7 were calculated to be 256 μ g and 68 μ g respectively. Agarose gel electrophoresis demonstrated that the knock-down of β -catenin while using β -actin as a housekeeping gene could promote apoptosis of cancer cells. Also for knockdown of β -catenin, the gel showed a reduction in the density of β -catenin bands by around 20% as compared with the band of the housekeeping gene β -actin for Caco2 cells only. Finally the gel demonstrated a successful formation of a reversible complex of siRNA with f-SWCNT 14, with an all N/P ratios.

Suggestion for future work:

1. Quantify the amount of inhibited protein by the siRNA using western Blot.
2. Hybridize siRNA with both f-SWCNTs 13 & 14 and determine the effective ratio of hybridization.
3. Determine the percentage of inhibition of the antiapoptetic protein by the TRI-functionalized SWCNTs.
4. Determine the synergistic anticancer activity of both Dox and the siRNA in the Tri-functionalized SWCNTs.

References

1. Sudhakar, A., *History of Cancer, Ancient and Modern Treatment Methods*. *J Cancer Sci Ther*, 2009. **1**(2).
2. Ruddon, R.W., *Cancer Biology*.
3. **Cell Division and Cancer**. Nanotechnology. 2015.
4. Devi, P.U., **BASICS OF CARCINOGENESIS**. Health Administrator. **XVII**(1): p. 16-24.
5. 5. F. William Orr, M.R.B., Leonard Weiss, **Microcirculation in Cancer Metastasis**. 1991.
6. Faltas, B., **Cornering metastases: Therapeutic targeting of circulating tumor cells and stem cells**. *Frontiers in Oncology*, 2012.
7. Naoyo Nishida, 2 Hirohisa Yano,1 Takashi Nishida,3 Toshiharu Kamura,2 and Masamichi Kojiro1, **Angiogenesis in Cancer**. *PMC*, 2006. **2**(3): p. 213–219.
8. Folkman, J., **Angiogenesis in cancer, vascular, rheumatoid and other disease**. *Nature medicine*, 1995. **1**(1): p. 27-30.
9. Eberhard, A., et al., **Heterogeneity of angiogenesis and blood vessel maturation in human tumors: implications for antiangiogenic tumor therapies**. *Cancer Research*, 2000. **60**(5): p. 1388-1393.

10. Iyer, A.K., et al., **Exploiting the enhanced permeability and retention effect for tumor targeting**. *Drug discovery today*, 2006. **11**(7): p. 812-818.
11. K1, G., **Enhanced permeability and retention (EPR) effect for anticancer nanomedicine drug targeting**. *Send to Methods Mol Biol*, 2010. **624**: p. 25-37.
12. **Multifunctional polymeric micelles for delivery of drugs and siRNA**. *Frontiers in Pharmacology* 2014. **5**(77).
13. Naidu, **Community Health Nursing**. 2009.
14. **Radiation in Medicine: A Need for Regulatory Reform**. 1996.
15. Mason., A.J.P.J.B.-L.M.D., **Hormonal therapy in cancer**. elsevier, 2004. **32**(3).
16. Ulrich, C.M., J. Bigler, and J.D. Potter, **Non-steroidal anti-inflammatory drugs for cancer prevention: promise, perils and pharmacogenetics**. *Nature Reviews Cancer*, 2006. **6**(2): p. 130-140.
17. Skarin, A., **Diagnosis In Oncology**. *journal of clinical oncology*.
18. Nurgalieva Z1, L.C., Du XL., **Chemotherapy use and risk of bone marrow suppression in a large population-based cohort of older women with breast and ovarian cancer**. *Med Oncol.* , 2011. **28**(3): p. 716–725.

19. Arvin, L.R.a.A., **Chemotherapy-induced immunosuppression.** Environ Health Perspect, 1982. **43**: p. 21–25.
20. Chow, E.K.H.a.D.H., **Cancer Nanomedicine: From Drug Delivery to Imaging.** Science Translational Medicine, 2013. **5**(216): p. 216rv4-216rv4.
21. Trafton, A., **Tumors Targeted Using Tiny Gold Particles.** MIT Tech Talk., 2009. **53**: p. 4-4.
22. Wakaskar, R.R., *Passive and Active Targeting in Tumor Microenvironment.* International Journal of Drug Development and Research, 2017. **9**(2).
23. Saltzman, W.M.J.H.T., Vladimir P, **Drug delivery systems.** AccessScience, 2008.
24. REMON BAZAK, M.H., 2 SAMAR EL ACHY,3 WAEL HUSSEIN,1 and TAMER REFAAT4,5, **Passive targeting of nanoparticles to cancer: A comprehensive review of the literature.** Molecular and Clinical Oncology, 2014. **2**(6): p. 904–908.
25. Wakaskar*, R.R., *Passive and Active Targeting in Tumor Microenvironment.* International Journal of Drug Development and Research, 2017. **9**(2).
26. Mohyeddin Assali1, A.N.Z., Naim Kittana2, Deema Hamad1 and Johnny Amer2, **Covalent functionalization of SWCNT with combretastatin A4 for cancer therapy.** . Nanotechnology, 2018. **29**(24).

27. S Mitra, U.G., P.C Ghosh, A.N Maitra, ***Tumour targeted delivery of encapsulated dextran–doxorubicin conjugate using chitosan nanoparticles as carrier.*** *Journal of Controlled Release*, 2001. **74**(1-3): p. 317-323.
28. Qixia Pan, Y.L., Gareth R.Williams, Lei Tao, Huihui Yang, Heyu Li, Limin Zhua, **Lactobionic acid and carboxymethyl chitosan functionalized graphene oxide nanocomposites as targeted anticancer drug delivery systems.** *ALSEVIER*, 2016. **151**: p. 812-820.
29. Tan, S.B.Z.Z.T.C.L.W.C.L.T.F.W., **A Focus on Nanoparticles as a Drug Delivery System.** *Nanomedicine: Nanotechnology, Biology and Medicine*, 2012. **7**(8): p. 1253-1271.
30. He, Q.L., et al., **Targeted delivery and sustained antitumor activity of triptolide through glucose conjugation.** *Angewandte Chemie*, 2016. **128**(39): p. 12214-12218.
31. A.Alqdeimata, A.M.K.H.T. and S. more, **A targeted drug delivery system of anti-cancer agents based on folic acid-cyclodextrin-long polymer functionalized silica nanoparticles.** *Journal of Drug Delivery Science and Technology* 2017. **41**: p. 367-374.
32. Yang, T., et al., **Targeted delivery of a combination therapy consisting of combretastatin A4 and low-dose doxorubicin against tumor neovasculature.** *Nanomedicine: Nanotechnology, Biology and Medicine*, 2012. **8**(1): p. 81-92.

33. Li Li*, R.Z., Wenyi Gu, Zhi Ping Xu*, **Mannose-conjugated layered double hydroxide nanocomposite for targeted siRNA delivery to enhanced cancer therapy.** *Nanomedicine: Nanotechnology, Biology, and Medicine*, 2017. **14**(7): p. 2355-2364.
34. Soni N1, S.N., Pandey H1, Maheshwari R2, Kesharwani P3, Tekade RK4., *Augmented delivery of gemcitabine in lung cancer cells exploring mannose anchored solid lipid nanoparticles.* *J Colloid Interface Sci*, 2016. **481**: p. 107-116.
35. Hergenrother, E.C.C.a.P.J., **Glucose conjugation for the specific targeting and treatment of cancer.** *chemical science*, 2013. **4**(6): p. 2319-2333.
36. Li, L., et al., **Mannose-conjugated layered double hydroxide nanocomposite for targeted siRNA delivery to enhance cancer therapy.** *Nanomedicine: Nanotechnology, Biology and Medicine*, , 2017.
37. Sato Y, B.E., Binding, *internalization, and degradation of mannoseterminated glucocerebrosidase by macrophages.* *J Clin Invest*, 1993. **91**(5): p. 1909-17.
38. Yin, L., et al., **Biodegradable Micelles Capable of Mannose-Mediated Targeted Drug Delivery to Cancer Cells.** *Macromolecular rapid communications*, 2015. **36**(5): p. 483-489.

39. de Mello LJ1, S.G., Winter E, Silva AH, Pittella F, Creczynski-Pasa TB, **Knockdown of antiapoptotic genes in breast cancer cells by siRNA loaded into hybrid nanoparticles.** *Nanotechnology*, 2017. **28**(17).
40. Li, J.-M., et al., **Multifunctional QD-based co-delivery of siRNA and doxorubicin to HeLa cells for reversal of multidrug resistance and real-time tracking.** . *Biomaterials*, 2012. **33**(9): p. 2780-2790.
41. Meng, H., et al. , **Engineered Design of Mesoporous Silica Nanoparticles to Deliver Doxorubicin and P-Glycoprotein siRNA to Overcome Drug Resistance in a Cancer Cell Line.** *ACS Nano*, 2010. **4**(8): p. 4539-4550.
42. Derek M. Dykxhoorn, C.D.N.P.A.S., **Killing the messenger: short RNAs that silence gene expression.** *Nature Reviews Molecular Cell Biology*, 2003. **4**: p. 457–467
43. Tim A. Rand, S.P., Fenghe Du, Xiaodong Wang, **Argonaute2 Cleaves the Anti-Guide Strand of siRNA during RISC Activation.** *Cell*, 2005. **123**(4): p. 621-629.
44. Angela Reynolds, D.L., Queta Boese, Stephen Scaringe, William S Marshall & Anastasia Khvorova, **Rational siRNA design for RNA interference.** *Nature Biotechnology* 2004. **22**: p. 326–330.
45. Kathryn A. Whitehead, R.L.D.G.A., **Knocking down barriers: advances in siRNA delivery.** *Nature Reviews Drug Discovery*, 2009. **8**: p. 129–138.

46. Conacci-Sorrell M, Z.J., Ben-Ze'ev A, ***The cadherin-catenin adhesion system in signaling and cancer.*** *J Clin Invest*, 2002. **109**(8): p. 987-91.
47. Giles RH, v.E.J., Clevers H. , **Caught up in a Wnt storm: Wnt signaling in cancer.** *Biochim Biophys Acta*, 2003. **1653**(1): p. 1–24.
48. Ikeda S, K.S., Yamamoto H, Murai H, Koyama S, Kikuchi A, **Axin, a negative regulator of the Wnt signaling pathway, forms a complex with GSK-3beta and beta-catenin and promotes GSK-3beta-dependent phosphorylation of beta-catenin.** *EMBO J.*, 1998. **17**(5): p. 1371-84.
49. Yost C, T.M., Miller JR, Huang E, Kimelman D, Moon RT, **The axis-inducing activity, stability, and subcellular distribution of beta-catenin is regulated in Xenopus embryos by glycogen synthase kinase 3.** *Genes Dev.*, 1996. **10**(12): p. 1443-54.
50. Cliffe A, H.F., Bienz M, **A role of Dishevelled in relocating Axin to the plasma membrane during wingless signaling.** *Curr Biol.*, 2003. **13**(11): p. 960-6.
51. R, N., **Cell biology: relays at the membrane.** *Nature.* , 2005. **438**(7069): p. 747-9.
52. Barbara Burtness, E.A.G., **Molecular determinants of head and neck cancer.** 2014.
53. Nithya Krishnamurthy, R.K., **Targeting the Wnt/beta-catenin pathway in cancer: Update on effectors and inhibitors.** *Cancer treatment reviews*, 2018. **62**: p. 50–60.

54. Goto M, M.R., Liu M, Lee J, Henson BS, Carey T, Bradford C, Prince M, Wang CY, Fearon ER, D'Silva NJ, **Rap1 stabilizes beta-catenin and enhances beta-catenin-dependent transcription and invasion in squamous cell carcinoma of the head and neck.** Clin Cancer Res., 2010. **16(1):** p. 65-76.
55. Tsai YP, Y.M., Huang CH, Chang SY, Chen PM, Liu CJ, Teng SC, Wu KJ, **Interaction between HSP60 and beta-catenin promotes metastasis.** Carcinogenesis, 2009. **30(6):** p. 1049-57.
56. E.Hagstrom, R.M.B., **Delivery of Small Interfering RNA to Mammalian Cells in Culture by Using Cationic Lipid / Polymer-Based Transfection Reagents.** Methods in Enzymology, 2005. **392:** p. 112-124.
57. Nouri Nayerossadat, T.M., and Palizban Abas Ali, **Viral and nonviral delivery systems for gene delivery.** Adv Biomed Res., 2012. **1.**
58. Cong-fei Xu, J.W., *Delivery systems for siRNA drug development in cancer therapy.* Asian Journal of Pharmaceutical Sciences, 2015. **10(1):** p. 1-12.
59. K.Y. Choi, M.S., S. Lee, X. Chen, **Protease-activated drug development.** Theranostics, 2012. **2:** p. 156-178.
60. V. Hornung, M.G.-B., C. Bourquin, et al., **Sequence-specific potent induction of IFN- α by short interfering RNA in plasmacytoid dendritic cells through TLR7.** Nat Med, 2005. **11:** p. 263-270.

61. A.D. Judge, V.S., J.R. Shaw, et al., **Sequence-dependent stimulation of the mammalian innate immune response by synthetic siRNA**. *Nat Biotechnol*, 2005. **23**: p. 457-462.
62. Ku, S.H., et al., **Tumor-Targeting Multifunctional Nanoparticles for siRNA Delivery: Recent Advances in Cancer Therapy**. . *Advanced Healthcare Materials*,, 2014. **3**(8): p. 1182-1193.
63. Iannazzo, D., et al., **Recent advances in carbon nanotubes as delivery systems for anticancer drugs**. . *Current medicinal chemistry*, 2013. **20**(11): p. 1333-1354.
64. Conniot, J., et al., **Cancer immunotherapy: nanodelivery approaches for immune cell targeting and tracking**. 2014. **2**(105).
65. Liu, Z., et al., **Carbon nanotubes in biology and medicine: In vitro and in vivo detection, imaging and drug delivery**. *Nano Research*, 2010. **2**(2): p. 85-120.
66. Kostarelos, K., A. Bianco, and M. Prato, **Promises, facts and challenges for carbon nanotubes in imaging and therapeutics**. *Nature Nanotechnology*, 2009. **4**(10): p. 627-633.
67. Zhang, Y., Y. Bai, and B. Yan, **Functionalized carbon nanotubes for potential medicinal applications**. *Drug Discovery Today*, 2010. **15** (11-13): p. 428-435.
68. Wu, H.-C., et al., **Chemistry of carbon nanotubes in biomedical applications**. *J. Mater. Chem.*, 2010. **20**(6): p. 1036-1052.

69. Lopez, C.F., et al., **Understanding nature's design for a nanosyringe.** Proceedings of the National Academy of Sciences, 2004. **101**(13): p. 4431-4434.

70. Allen, B.L., et al., *Mechanistic Investigations of Horseradish Peroxidase-Catalyzed Degradation of Single-Walled Carbon Nanotubes.* **Journal of the American Chemical Society**, 2009. **131**(47): p. 17194-17205.

71. Kagan, V.E., et al., **Carbon nanotubes degraded by neutrophil myeloperoxidase induce less pulmonary inflammation.** Nature Nanotechnology, 2010. **5**(5): p. 354-359.

72. Liu, Z., et al., **Carbon materials for drug delivery & cancer therapy.** Materials today, 2011. **14**(7): p. 316-323.

73. Angelikopoulos, P., et al., *Dispersing individual single-wall carbon nanotubes in aqueous surfactant solutions below the cmc.* **The Journal of Physical Chemistry C**, 2009. **114**(1): p. 2-9.

74. Debnath, S., et al., *A study of the interaction between single-walled carbon nanotubes and polycyclic aromatic hydrocarbons: toward structure–property relationships.* **The Journal of Physical Chemistry C**, 2008. **112**(28): p. 10418-10422.

75. Gao, J., et al., **Selective wrapping and supramolecular structures of polyfluorene–carbon nanotube hybrids.** ACS nano, 2011. **5**(5): p. 3993-3999.

76. Zhao, Y.-L.a.J.F., **Noncovalent functionalization of single-walled carbon nanotubes.** *Accounts of chemical research.* Stoddart, 2009. **42(8):** p. 1161-1171.

77. Prencipe, G., et al., *PEG branched polymer for functionalization of nanomaterials with ultralong blood circulation.* *Journal of the American Chemical Society*, 2009. **131(13):** p. 4783-4787.

78. Guldi, D.M., et al., *Supramolecular Hybrids of [60] Fullerene and Single-Wall Carbon Nanotubes.* *Chemistry-A European Journal*, 2006. **12(15):** p. 3975-3983.

79. Yang, K., L. Zhu, and B. Xing., *Adsorption of polycyclic aromatic hydrocarbons by carbon nanomaterials.* *Environmental science & technology*, 2006. **40(6):** p. 1855-1861.

80. Assali, M., et al., **Non-covalent functionalization of carbon nanotubes with glycolipids: glyconanomaterials with specific lectin-affinity.** *Soft Matter*, 2009. **5(5):** p. 948-950.

81. Kushwaha, S.K.S., et al., *Carbon nanotubes as a novel drug delivery system for anticancer therapy: a review.* *Brazilian Journal of Pharmaceutical Sciences*, 2013. **49(4):** p. 629-643.

82. Bahr, J.L., et al., *Functionalization of carbon nanotubes by electrochemical reduction of aryl diazonium salts: a bucky paper electrode.* *Journal of the American Chemical Society*, 2001. **123(27):** p. 6536-6542.

83. Wu, H.-C., et al., *Chemistry of carbon nanotubes in biomedical applications*. **J. Mater. Chem**, 2010. **20**(6): p. 1036-1052.
84. Tagmatarchis, N.a.M.P., *Functionalization of carbon nanotubes via 1, 3-dipolar cycloadditions*. **Journal of materials chemistry**, 2004. **14**(4): p. 437-439.
85. Zamolo, V.A., E. Vazquez, and M. Prato, **Carbon Nanotubes: Synthesis, Structure, Functionalization, and Characterization**. Polyarenes II-springer, 2013: p. 65-109.
86. Rao, C.N.R., et al., **Nanotubes**. **Chem Phys Chem**, 2001. **2**(2): p. 78-105.
87. Dyke, C.A.a.J.M.T., *Solvent-free functionalization of carbon nanotubes*. **Journal of the American Chemical Society**., 2003. **125**(5): p. 1156-1157.
88. **Doxorubicin Hydrochloride**. 2019.
89. **Doxorubicin**. . [cited 2019 Mar, 1] [cited 2019 Mar 1]; Available from: Available from: <https://www.drugbank.ca/drugs/DB00997>.
90. Vos, K.J., et al., *A multi-compartment pharmacokinetic model of the interaction between paclitaxel and doxorubicin*. **EPJ Nonlinear Biomedical Physics**, 2014. **2**(1): p. 13.
91. **Doxorubicin**. [cited 2017 Dec, 9].

92. Mobaraki, M., et al., *Molecular Mechanisms of Cardiotoxicity: A Review on Major Side-effect of Doxorubicin*. **Indian Journal of Pharmaceutical Sciences**, 2017. **79**(3).
93. Kratz, F., **Acid-sensitive prodrugs of doxorubicin**. Anthracycline chemistry and biology II, Springer, 2007: p. 73-97.
94. Bae, Y., et al., **Multifunctional polymeric micelles with folate-mediated cancer cell targeting and pH-triggered drug releasing properties for active intracellular drug delivery**. *Molecular BioSystems*, 2005. **1**(3): p. 242-250.
95. Mohyeddin Assali, N.K., Safa' Raed Dayyeh, **Dual functionalization of single-walled carbon nanotubes for targeted cancer therapy**, in **Graduate Studies**. 2018, An-Najah National University.
96. Xun Sun, S.C., Jianfeng Han, Zhirong Zhang, *Mannosylated biodegradable polyethyleneimine for targeted DNA delivery to dendritic cells*. **International Journal of Nanomedicine**, 2012. **7**: p. 2929–2942.
97. NaJung Kima, Dahai Jiangb,1, Ashley M. Jacobic, Kim A. Lennox, Scott D. Rosec, Mark A. Behlke, and b. Aliasger K. Salema, *, *Synthesis and characterization of mannosylated pegylated polyethylenimine as a carrier for siRNA*. **International Journal of Pharmaceutics**, 2012. **427**: p. 123– 133.

98. Zahra Ali Mohammadi a, S.F.A.a., *, Ali Zarrabi b, Mohammad Reza Talaie, **A comparative study on non-covalent functionalization of carbon nanotubes by chitosan and its derivatives for delivery of doxorubicin.** *Chemical Physics Letters*, 2015. **642**: p. 22–28.
99. Assali, M., et al., *Single-walled carbon nanotubes-ciprofloxacin nanoantibiotic: strategy to improve ciprofloxacin antibacterial activity.* **International Journal of Nanomedicine**, 2017. **12**: p. 6647-6659.
100. Ashwell, G., **Colorimetric analysis of sugars.** 1957.
101. Scott Jr, T.A.a.E.H.M., **Determination of dextran with anthrone.** *Analytical Chemistry*, 1953. **25**(11): p. 1656-1661.
102. Patri, J.D.C.K., **Characterization of Nanoparticles Intended for Drug Delivery.** Vol. 697. 2010, *Methods in Molecular Biology*. 63-70.

جامعة النجاح الوطنية

كلية الدراسات العليا

التفعيل المتعدد لأنابيب الكربون النانوية أحادية الجدران القائم على
الايصال المشترك لجين مثبط مع دوكسيروبيسن لموازرة النشاط
المضاد للسرطان

إعداد

نورا سامي يوسف غزال

إشراف

د. محي الدين العسالي

د. نعيم كتانة

قدمت هذه الأطروحة استكمالاً لمتطلبات الحصول على درجة الماجستير في العلوم الصيدلانية،
بكلية الدراسات العليا، في جامعة النجاح الوطنية، نابلس - فلسطين.

2019

ب

التفعيل المتعدد لأنابيب الكربون النانوية أحادية الجدران القائم على الايصال المشترك لجين

مثبط مع دوكسيروبيسن لموازرة النشاط المضاد للسرطان

إعداد

نورا سامي يوسف غزال

إشراف

د. محي الدين العسالي

د. نعيم كتانة

الملخص

العلاج الكيميائي هو استراتيجية أساسية في علاج السرطان. لكنها تؤثر على الخلايا السليمة مثل الخلايا السرطانية مما يؤدي إلى عدد من الآثار الجانبية الشديدة. لذلك، يتوق العديد من الباحثين إلى تطوير أنظمة جديدة لتوصيل الأدوية قد تساعد في تقليل الجرعات المستخدمة وتقليل الآثار الجانبية. لذلك تم تطبيق العديد من الجهود لتطوير أنظمة توصيل الأدوية القائمة على أنابيب الكربون النانوية. الهدف من هذا البحث هو تطوير نظام نانوي جديد مضاد للسرطان يعتمد على التفعيل المتعدد لأنابيب الكربون النانوية أحادية الجدران من خلال ربط مركب متعدد الأمينات وعامل استهداف وهو سكر المنوز مع انابيب الكربون النانوية أحادية الجدران من خلال رابطة تساهمية و بالإضافة الى ربط دواء الدوكسوروبيسن من خلال رابطة غير تساهمية على سطح انابيب الكربون النانوية أحادية الجدران.

وأظهر تحليل الدواء النانوي بواسطة المجهر الالكتروني النافذ فصل وتوزع جيد لأنابيب النانوية التي تشير إلى النجاح الوظيفي . بالإضافة الى ذلك، تم تحديد كفاءة التفعيل لأنابيب الكربون النانوية بواسطة جهاز التحليل الحراري الذي أظهر 77.5% نسبة التحميل الكامل لأنابيب الكربونية النانوية. وشحنة السطح المفعلة كانت +28 ملفولت لمركب 13 و +47 ملفولت لمركب 14 كما تم تأكيده بجهاز تحليل جهد زيتا.

أما فيما يخص دراسة تأثير السمية والنشاط المضاد للسرطان، تمت الدراسة للمركبات المذكورة أعلاه، بتراكيز وظروف مختلفة. ولوحظ انه يسبب تسمماً خلويًا أكبر عند درجات الحموضة الذي تم اختباره عليها، مع وجود أعلى سمية عند تركيز 4 ميكروغرام / مل عند درجة الحموضة 6.5 لمركب 14.

أما بالنسبة لدراسة الانتقائية لمستقبل المنوز، فقد قلت نسبة السمية بحوالي 96-98% بعد الاحتضان المسبق للمنوز بتراكيز مختلفة، مما يشير أن دخول هذا المركب يعتمد على نسبة مستقبلات المنوز الفعالة، مما يضيف نوعاً من الانتقائية للخلايا السرطانية مقارنة بالخلايا الطبيعية.

في حالة خلايا (caco2)، توضح ان عملية تثبيط جين β -catenin لها اثر ايجابي في اضعاف الخلايا السرطانية بالاعتماد على β -actin كقيم مرجعيه، بحيث تظهر النتائج انه تم تثبيطه بنسبه 20% مقارنة مع β -actin.

اخيراً، أظهر الجل ارتباطاً ناجحاً بين المركب 14 والجين المثبط عند جميع نسب (N/P) التي تم العمل عليها.

